



CrossMark
click for updates

Review

Cite this article: Shyy W, Kang C-k, Chirarattananon P, Ravi S, Liu H. 2016 Aerodynamics, sensing and control of insect-scale flapping-wing flight. *Proc. R. Soc. A* **472**: 20150712. <http://dx.doi.org/10.1098/rspa.2015.0712>

Received: 15 October 2015

Accepted: 4 January 2016

Subject Areas:

biomechanics

Keywords:

biomimicry, flapping flight, insect scale

Author for correspondence:

Wei Shyy

e-mail: weishyy@ust.hk

Aerodynamics, sensing and control of insect-scale flapping-wing flight

Wei Shyy¹, Chang-kwon Kang²,
Pakpong Chirarattananon³, Sridhar Ravi^{4,5}
and Hao Liu^{5,6}

¹Department of Mechanical and Aerospace Engineering, Hong Kong University of Science and Technology, Clear Water Bay, Hong Kong

²Department of Mechanical and Aerospace Engineering, University of Alabama in Huntsville, Huntsville, AL, USA

³Department of Mechanical and Biomedical Engineering, City University of Hong Kong, Kowloon Tong, Hong Kong

⁴Graduate School of Engineering, Chiba University, Chiba, Japan

⁵School of Aerospace, Mechanical and Manufacturing Engineering, RMIT University, Melbourne, Victoria, Australia

⁶Shanghai-Jiao Tong University and Chiba University International Cooperative Research Centre (SJTU-CU ICRC), Minhang, Shanghai, China

There are nearly a million known species of flying insects and 13 000 species of flying warm-blooded vertebrates, including mammals, birds and bats. While in flight, their wings not only move forward relative to the air, they also flap up and down, plunge and sweep, so that both lift and thrust can be generated and balanced, accommodate uncertain surrounding environment, with superior flight stability and dynamics with highly varied speeds and missions. As the size of a flyer is reduced, the wing-to-body mass ratio tends to decrease as well. Furthermore, these flyers use integrated system consisting of wings to generate aerodynamic forces, muscles to move the wings, and sensing and control systems to guide and manoeuvre. In this article, recent advances in insect-scale flapping-wing aerodynamics, flexible wing structures, unsteady flight environment, sensing, stability and control are reviewed with perspective offered. In particular, the special features of the low Reynolds number flyers associated with small sizes, thin and light structures, slow flight

with comparable wind gust speeds, bioinspired fabrication of wing structures, neuron-based sensing and adaptive control are highlighted.

1. Introduction

There are nearly a million species of flying insects. Of the non-insects, another 13 000 warm-blooded vertebrate species, including mammals, about 9000 birds and 1000 bats, have taken to the skies [1]. In parallel, human-engineered flapping-wing-based micro air vehicles (MAVs) have been actively investigated in the last two decades or so, and can revolutionize our capabilities in areas such as environmental monitoring and surveillance and security. Compared to flapping wings, conventional aeroplanes with fixed wings are relatively simple. The forward motion relative to the air causes the wings to generate lift, with the thrust being produced by the engine. In biological flight, the wings not only move forward relative to the air, they also flap up and down, plunge and sweep [2–5], so that both lift and thrust can be generated and balanced in accordance with the instantaneous flight task. By increasing the wing speed relative to the air while adjusting the effective angle of attack (AoA), natural flyers generate sufficient lift, accommodate uncertain surrounding environment and offer superior flight stability and dynamics with highly varied speeds and missions.

As the size of a flyer is reduced, the wing-to-body mass ratio tends to decrease as well. Figure 1 illustrates such a trend and some of the major implications via the relationship between the Reynolds number and wingbeat frequency. The Reynolds number, defined as $Re = U_{ref}L/v$, where U_{ref} and L are the characteristic velocity and length scales, respectively, and v is the kinematic viscosity of air and is an important dimensionless number in aerodynamics; it provides an indication of the relative magnitudes of the flow inertia and viscous effects [6]. The wings of large birds such as ospreys, kites and eagles account for 20% or more of their body weight. As the size of the flyer is reduced, the Reynolds number and the wing/body mass ratio decrease in general, while the flapping frequency increases.

Those with a higher wing-to-body mass ratio and moment of inertia, such as bats and butterflies, are more manoeuvrable, capable of making abrupt changes of trajectories within a time comparable to that of a flapping cycle. Their larger inertia make the flyers capable of making turns within one or two flapping periods. However, they pay a penalty for this ability because a heavier wing consumes more energy while flapping. With the flapping and body response time scales being comparable, the flyer's flight dynamics and control need to be closely linked to the instantaneous aerodynamics, because the time history of the flapping-wing aerodynamics directly affects a flyer's performance characteristics.

Many small flyers with lower wing-to-body mass ratio, such as hummingbirds and insects (with butterflies as a notable exception), tend to have much faster flapping time scales than their bodies' response time scale. The lift, drag and thrust variations during the flapping cycle tend to be smoothed out over the entire flight flapping cycles. However, this does not mean that the flapping-wing aerodynamics of small flyers can simply be considered as quasi-steady.

In this article, recent advances in flapping-wing aerodynamics, flexible wing structures, unsteady flight environment, sensing, stability and control associated with flapping-wing flight, focusing on insect-scale issues, are reviewed with perspective offered.

2. Key scaling parameters of flapping wing aerodynamics

Scaling laws are useful to reduce the number of parameters, to clearly identify characteristic properties of the system under consideration and to indicate which combination of parameters becomes important under a given condition [7–9]. In flapping-wing flight, three-dimensionless parameters (table 1) are often used to relate the fluid dynamics and wing kinematics to

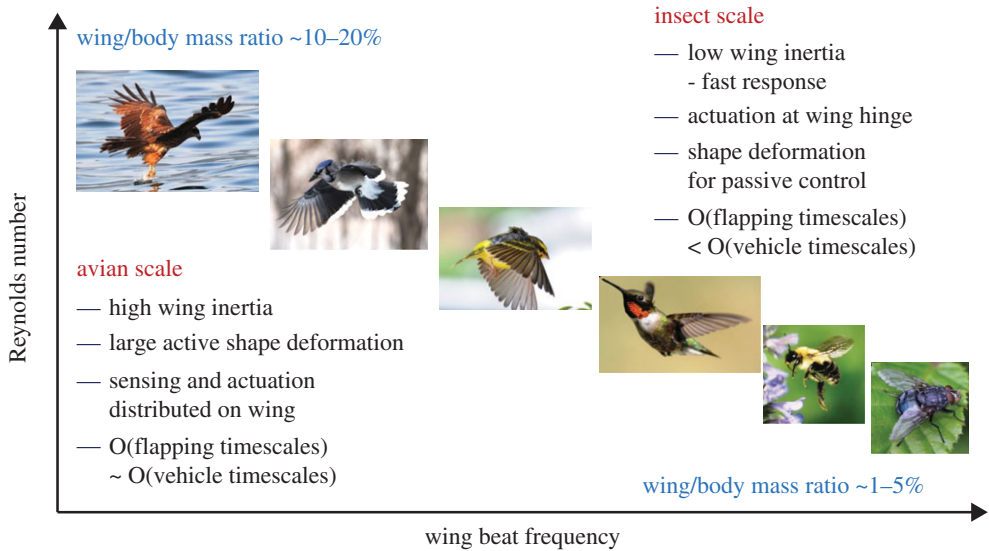


Figure 1. Characteristics of biological flapping flight based on the Reynolds number, flapping frequency and wing/body mass ratio.

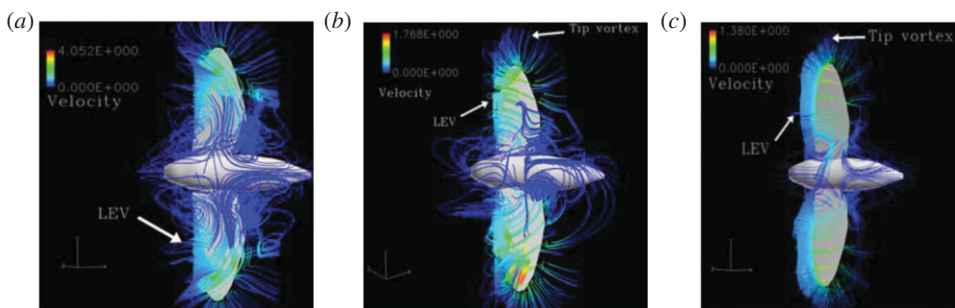


Figure 2. Numerical results of LEV structures at different Reynolds numbers. Adapted from [10]. (a) Hawkmoth, $Re = 6000$, (b) fruit fly, $Re = 120$ and (c) thrips, $Re = 10$.

Table 1. Dimensionless parameters in a flapping-wing system.

dimensionless parameter	symbol	definition
Reynolds number	Re	$U_{ref}L/\nu$
reduced frequency	k	fL/U_{ref}
Strouhal number	St	$2fh_a/U_{ref}$

the resulting force coefficients. Other dimensionless parameters relevant to the fluid–structure interaction are highlighted in §4c.

Most insects and birds fly in the Reynolds number regime between $O(10^1)$ and $O(10^4)$. At these low Reynolds numbers, both viscous and inertia effects are important and the flow is characterized by unsteady large vortical flow structures. The structure and stability of large coherent vortices, forming a well-identified lower pressure core to help enhance lift, are highly influenced by the Reynolds number [10,11]. At the hawkmoth scale of $Re = 6000$, the leading-edge

vortex (LEV), the large vortical structure near the leading-edge of the wing, is intense, conical with significant spanwise flow at the core, and breaks down at 75% of the span (figure 2a). At $Re = 120$, relevant for fruit flies, the LEV is connected to the wing tip vortex (TiV) and the spanwise flow is weaker (figure 2b). At the thrips scale of $Re = 10$, the LEV is cylindrical and uniform along the wing span (figure 2c).

The reduced frequency k is a measure of unsteadiness that compares the spatial wavelength of the flow disturbance to the chord [12]; it gives the ratio between the fluid convection time scale, L/U_{ref} , and the motion time scale, $1/f$, where f is the flapping frequency. In forward flight, the reduced frequency and the wingbeat amplitude tend to be low, between 0.1 and 0.3 [1].

The Strouhal number indicates the ratio between the reference velocity and flapping speed based on the peak-to-peak amplitude. It characterizes the dynamics of the wake and shedding behaviour of vortices of a flapping wing in forward flight [12,13]. For a family of two-dimensional wakes of oscillating foils in water [14], the Strouhal number range between $0.25 < St < 0.35$ was found to be efficient [13,15,16]. Moreover, insects, birds and bats flap their wings in a similar range $0.2 < St < 0.4$ in forward flight [17]. The Strouhal number is also associated with the optimal vortex formation in biological propulsion [18].

3. Rigid flapping-wing aerodynamics

(a) Unsteady lift enhancement mechanisms

Natural flyers use flapping mechanisms to generate lift and thrust. These mechanisms are related to formation and shedding of the vortices into the flow, varied wing shape and structural flexibility [1].

The earliest unsteady lift generation mechanism to explain how insects fly, found by Weis-Fogh [19], was the clap-and-fling motion of a chalcid wasp, *Encarsia formosa*. The relative benefit of clap-and-fling lift enhancement strongly depended on stroke kinematics and could potentially increase the performance by reducing the power requirements [20,21]. The clap-and-fling mechanism is beneficial in producing a mean lift coefficient to keep a low weight flyer aloft. Numerous natural flyers, such as hawkmoths, butterflies, fruit flies, wasps and thrips enhance their aerodynamic force production with the clap-and-fling mechanism [19,22–25].

At the end of each stroke, flapping wings often experience rapid pitching rotation, which can enhance the aerodynamic force generation [26]. The phase difference between the translation and the rotation can be used as a lift controlling parameter. Similar to the Magnus effect, if the wing flips before a stroke ends, then the wing undergoes rapid pitch-up rotation in the favourable translational direction enhancing the lift. This is called the advanced rotation. On the other hand, in delayed rotations, if a wing rotates back after the stroke reversal, then when the wing starts to accelerate, it pitches down resulting in reduced lift [26]. The lift peak at the stroke ends was shown to be proportional to the angular velocity of the wing using the quasi-steady theory [27].

The wake capture mechanism is often observed during a wing-wake interaction. When the wings reverse their translational direction, the wings meet the wake created during the previous stroke, by which the effective flow velocity increases and additional aerodynamic force peak is generated [1,26,28–32]. The effectiveness of the wake capture mechanism is also a function of wing kinematics and flow structures around the flapping wings.

The delayed stall of LEV can significantly promote lift associated with a flapping wing [33–35]. The LEV creates a region of lower pressure above the wing and hence it would enhance lift. When a flapping wing travels several chord lengths, the flow separates from the leading and trailing edges, as well as at the wing tip, and forms large organized vortices known as a LEV, a trailing edge vortex, and a TiV (figure 3). In hover, however, depending on the specific kinematics, the TiVs could either promote or make little impact on the aerodynamics of a low aspect ratio flapping wing [32]. As detailed in Shyy *et al.* [1,36], for $Re = O(10^2)$, corresponding to the small insect flight regime, investigations of the aerodynamic performances associated with various wing geometry and flapping kinematics showed that there is significant variance in the spanwise distribution

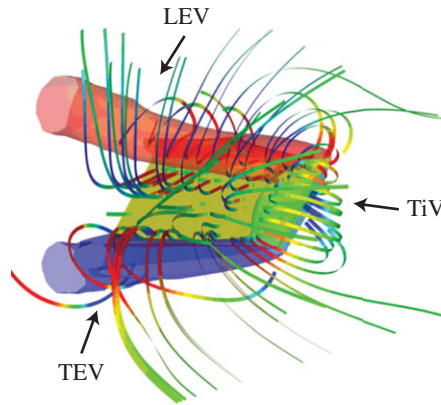


Figure 3. Vortical flow structures around a low aspect ratio flapping wing. Spanwise vorticity iso-surfaces are coloured by the vorticity magnitude. Streamlines are coloured with the horizontal velocity magnitude.

of forces for three-dimensional wings. Wing motions with a prominent TiV exhibit significant variations along the span. Furthermore, kinematics with low angles of attack that suppress the TiV generation, appear to have a relatively constant response along the span. According to the classical stationary wing theory [37], a three-dimensional low aspect ratio wing experiences a lower lift than its two-dimensional counterpart due to the downwash associated with TiVs. In unsteady flow around a hovering wing, however, the TiVs can contribute to lift generation rather than just drag generation on the wing [31].

The LEV is common and important to the flapping-wing aerodynamics at the Reynolds number of $O(10^4)$ or lower, which corresponds to the hummingbird and insect flight regimes. However, the LEV structures and distribution of spanwise flow inside the LEV change with the variation of Reynolds number (wing sizing, flapping frequency, etc.) and with the interactions between LEVs and TiVs and hence influence the aerodynamic force generation, see also §2. The stability of the prolonged attachment of the LEV on the wing is also related to the convection of momentum along the spanwise direction [11]. The LEV as a lift enhancement mechanism for flapping wing at Reynolds number of $O(10^5-10^6)$ seem less certain because, as pointed out in [38], a dynamic-stall vortex on an oscillating aerofoil is often found to break away and to convect elsewhere as soon as the aerofoil translates. More comprehensive review of the unsteady lift enhancement mechanisms can be found in [1,30,39].

(b) Tandem and corrugated wings

For many insects, four winged with two pairs of fore and hindwings are observed and wing-wing interactions play an important role in aerodynamics and stability. In *Lepidoptera*, which includes butterflies and moths, the fore and hindwings usually flap in sync. For some moths, the fore and hindwings are even mechanically coupled [40], whereas butterflies can control the wings individually [41]. Butterflies are known to be anteromotoric, driven primarily by forewings [42]. Most studies of *Lepidoptera* analyse their wings as a whole, instead of analysing fore and hindwings separately and the effects of the wing-wing interaction for butterflies are still not well understood.

Dragonflies also have two pairs of fore and hindwings with relatively high aspect ratio. They can glide, flap and hover while showcasing amazing manoeuvring abilities. Dragonflies are one of the fastest insects with good manoeuvrability [43]. The phase difference between the fore and hindwing motions is known to be one of the keys of dragonflies' flight characteristics. By optimizing wing-wing interaction, dragonflies can enhance the aerodynamic efficiency [43,44] and improve gust resistance [43]. For example, while cruising, dragonflies' fore and hindwings are

out of phase to attain better flight efficiencies [45]. The interaction between the fore and hindwings is highly affected by the wake structures produced by both wings [46]; while the wing–vortex interaction can lead to increased lift and thrust [43,47], it can also be detrimental to lift due to downwash [48,49]. The flapping motions are in reduced phase shift to generate large magnitude forces and accelerations during manoeuvres [50–52]. One major deficiency of the literature to date is that the wings are considered to be rigid wings and smooth without accounting for the intrinsic structural flexibility and corrugation [53]. Both structural flexibility and corrugation can substantially affect the nearwing wake structure and resulting aerodynamic forces [1].

Another issue is the connection between the wing phasing and the effective wing aspect ratio. For example, the dragonfly, *Sympetrum sanguineum* [54], has an aspect ratio of 9.54 for its forewing and 6.94 for its hindwing. When the wings operate in close proximity, functioning as one low aspect ratio wing while neglecting the gap between the fore and hindwings, the aspect ratio changes to 4.18, which is less than half of the aspect ratio of the forewing. For out of phase flapping, they operate with two pairs of high aspect ratio wings, which interact with each other to produce a more complex flow phenomenon and harvest additional energy by removing excess swirl from the wake [44,55]. On the other hand, in the case of in phase flapping, when dragonflies execute high energy demand flight manoeuvres or take-off [51], the wings operate in close proximity, which essentially can be considered as one low aspect ratio wing. The flow structures associated with these different flapping modes are highlighted by Fu *et al.* [55].

While conventional aerofoils are smooth and streamlined, insect wings exhibit rough surfaces, e.g. the cross-sectional corrugations of dragonfly wings or scales on the wing surface of butterfly and moth. It is suggested that corrugated wing configuration can help the aerodynamic performance and stability of the wing's ultralight construction [1,43,56–64]. However, the detailed physical mechanisms accounting for a corrugated wing's influence on its aerodynamics is still to be further investigated [57]. The conventional view is that vortices fill the profile valleys formed by these bends and therefore smooth the profile geometry [59]; other investigations [43,60,61] suggest that a smooth rigid flat plate may aerodynamically perform better than a corrugated wing.

(c) Quasi-steady models of flapping-wing aerodynamics

Early analyses in flapping-wing aerodynamics have used actuator disc models from helicopter theories to estimate lift on insect wings [65] based on the parallels that exist between flapping wing and rotary wing flight. Both use a self-generated wing motion to create lift. Both tilt the stroke/rotational planes forward in order to generate propulsive forces. However, the direct application of helicopter theory in flapping-wing aerodynamics ignores the essential feature of flapping as a reciprocating and intermittent lifting and propulsion mechanism, in which the generated forces result from an unsteady momentum flux [66].

To model the lift and drag as a function of time for flapping wings, unsteady linearized theories and quasi-steady models for pitching and plunging aerofoils [67–69] are often applied to insect flapping-wing aerodynamics. Since the associated flow is unsteady, a quasi-steady model based on the nominal position and angles of a wing relative to undisturbed freestream does not capture the main physics properly. An adjusted quasi-steady model by correcting the surrounding flow parameters including the effective AoA and associated flow structures such as jet flows, can perform much better. By assuming that the instantaneous aerodynamic forces depend on the instantaneous velocity and acceleration of the wing motion, these quasi-steady models provide a closed form formulation for the delayed stall, rotational circulation and added mass [26,27,70,71] including passively rotating wings [72] and chordwise flexible aerofoils [73].

A quasi-steady model can be valuable if a proper account can be given to address the effects of wing kinematics on the delayed stall and other unsteady mechanisms [26]. Such an approach often under-represent, for example, the influence from the nonlinear wing–wake interaction relevant in certain cases [26,74]. A fundamental limitation of these simplified models is the lack of information of the key physical parameters, such as the lift coefficient as a function of AoA while

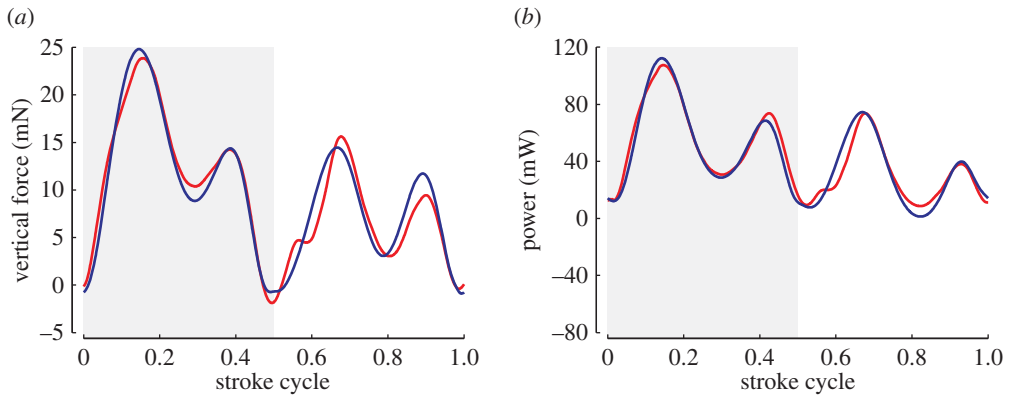


Figure 4. Comparison of (a) aerodynamic lift and (b) power. Navier–Stokes informed hybrid quasi-steady model (blue); Navier–Stokes equation solution (red). Adapted from [78].

the wing undergoes unsteady motions [26] and aerodynamic [75] or aeroelastic [73] damping coefficients. These coefficients are empirically determined from various experiments [26,27,73,76]. Such a need for empirically fitted coefficients can be partially mitigated by considering an unsteady model that captures the nonlinear effect of the LEV on the lift [77] or a hybrid model of high-fidelity Navier–Stokes equation solutions and low-order quasi-steady models [78]. Nevertheless, it is important that a first principle-based framework be established. By fitting the coefficients in the quasi-steady models to the solutions from the high-fidelity Navier–Stokes equations, an efficient yet accurate solution can be obtained even for a complex three-dimensional flapping-wing motion as illustrated in figure 4.

4. Aeroelastic wing dynamics

Birds, bats and insects flex their wings to change the wing shape and area during flight either actively or passively. Since the aerodynamic force depends on the wing area, an increase in the projected area due to wing deformation can lead to a performance enhancement [36]. On the other hand, bat wings are made of a thin membrane supported by the arm and finger bones. Due to the stretchiness, bats wing membranes can deform only marginally, reducing the span by about 20%. When the forward speed exceeds a critical value, the flexible wings can spontaneously start to flap, enhancing the lift due to an attached LEV during the downstroke [79], accompanied by a higher drag. However, over-flexing wings can lead to inefficient aerodynamic performance [1].

Insect wings, much smaller and thinner than bird and bat wings, can substantially deform during flight due to the structural flexibility instead of active manipulation. Their wing properties are anisotropic because of the membrane–vein structures [1]. The wing thickness varies across span and chord. Moreover, the wing motion is three-dimensional with a wing rotation at the wing root. The spanwise bending stiffness is about 1 to 2 orders of magnitude larger than the chordwise bending stiffness in a majority of insect species [80,81]. They exhibit substantial variations in aspect ratios and shapes, but share a common feature of a reinforced leading edge [81]. A dragonfly wing has more local variations in its structural composition and is more corrugated than the wing of a cicada or a wasp. The wing corrugation increases both warping rigidity and flexibility [82]; however, its aerodynamic effects are still not well understood [43]. Furthermore, studies of neuromuscular control indicate that flies can actively modulate stroke deviation by altering the activity of steering muscles [83,84]. While normal hovering with a nearly flat plane strokes are observed [19], most insects often exhibit U-shaped [85,86] or figure of eight motions [26,87]. The complex interplay between the kinematics of the wing, anisotropic wing structures and nonlinear unsteady aerodynamics makes the analysis of flapping-wing flyers extremely challenging, but also intriguing.

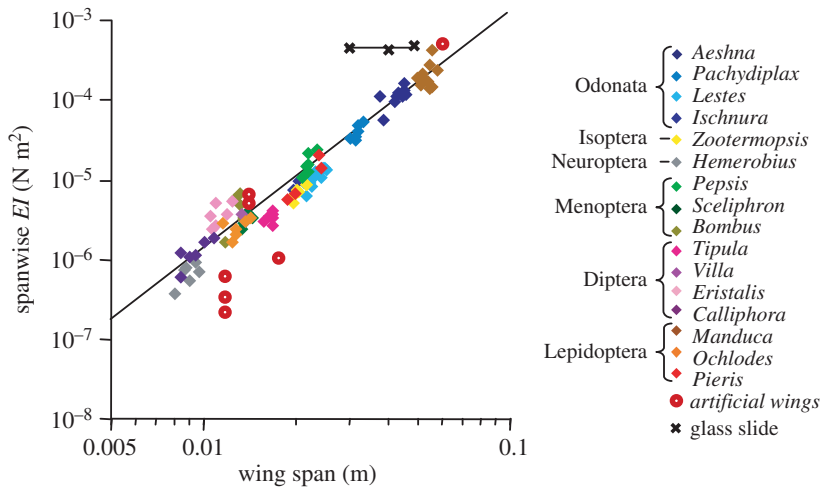


Figure 5. Spanwise flexural stiffness of various insect species versus wingspan from [80], overlaid by flexural stiffness of fabricated wings from [95–100]. Adapted from [80].

(a) Flexible wing design

Biological data and physics of scaling provide researchers with preliminary morphological parameters regarding the appropriate wing size, flapping frequency, and flight speed based on the projected size and weight of the vehicles [1,88]. The scaling of wing length follows from the concept of wing loading, the ratio of wing area over weight, which is determined by balancing of weight and lift in steady flight [1,89]. Based on mass and wingspan data from [89,90] covering a wide range of flying animals and machines, Liu suggests that, over a large range of the weight, the wing length of birds and aircraft basically follows the power law $m \propto R^{1/3}$ [91]. The proposed scaling law is consistent with the wingspan data [92] of flapping-wing insects, hummingbirds and robots at the small end of the spectrum. The best fit line across 25 species and five flight-capable robots is given as $R \propto m^{0.36}$. Similar physical arguments could be made regarding the flapping frequency. By considering the limit of muscle power, Pennycuik [93] bounds the maximum flapping frequency as $f_{\max} \propto m^{-1/3}$, whereas Shyy *et al.* [1] predicts the lower bound of flapping frequency from the lift requirement as $f_{\min} \propto m^{-1/6}$. Again, the predictions are in accordant with insects, hummingbirds and small flapping-wing robot data from [92] that indicates $f \propto m^{-0.22}$.

In addition to shape and size, aerodynamic performance of flying insects is highly dependent on deformation of the wings during flight. Owing to the absence of muscles at wing base, deformation of the insect wings in flight is primarily due to the couple between aerodynamic forces, wing structure and inertial [80,94]. Biological studies on multiple insect species reveal a strong correlation between wing flexibility (in both spanwise and chordwise directions, with the spanwise stiffness being 1–2 orders of magnitude larger than chordwise stiffness) and wingspan (figure 5) [80]. This indicates that shape, material density and wing flexibility are critical to aerodynamic performance. This information supplies researchers with basic design parameters for fabrication of artificial flapping wings.

Driven by the availability of examples from biology and the lack of comprehensive understanding of flapping-wing aerodynamics and aeroelasticity, a common approach in the design of artificial wings is to take inspiration from nature. Numerous fabricated wings were shaped after biological fliers, including ravens [101], bats [95], hawkmoths [102], dragonflies [88,103], butterflies [88], flies [104], hoverflies [96,105] and cicadas [106]. Simultaneously, vein geometry, wingframe and membrane materials are required to possess appropriate strength and stiffness. In one of the pioneering flapping-wing MAV prototypes [88], the authors mimicked the

wing design based on bat wings. Titanium alloy was chosen as material for the wingframe thanks to its ductile property and compatibility with the manufacturing process. Silicon was found to be too fragile and unable to withstand flapping motion as fast as 30 Hz and the high density of stainless steel rendered it unsuitable for the application.

In other flapping-wing devices, it is not uncommon to customize materials and wing geometry of fabricated wings to obtain desired physical properties [97,102]. Meng *et al.* [97] chose 40- μm -thick SU-8 as the material for the veins and the 7.5- μm thick polyimide as wing membrane for a 3.5 cm wingspan prototype. The resultant wings have the flexural stiffness comparable to dipteran insects [97]. Agrawal *et al.* [102] performed an extensive analysis on aerodynamic performance and wing deformation of synthetic hawkmoth wings constructed from different materials (carbon, nylon and rubber). Therein, the leading edge and trailing edge veins were optimized to achieve the desired deformation profile. A plot summarizing and comparing the spanwise stiffness of artificial wings and insect wings of various sizes is illustrated in figure 5.

With potential benefits to the aerodynamic performance [59], more recently, some researchers have explored three-dimensional wing designs with cambered and corrugated structures [96, 98,99]. In [96], hoverfly-like wing was designed and fabricated with 50–125- μm vein heights and 100- μm corrugation heights. The combination of veins and corrugations affects the wing deformation under different loading that are believed to play a role in lift and drag coefficients at low Reynolds number conditions [107]. Bioinspired wings in [99] were designed to feature microscale wrinkles similar to bird feathers. Compared to a flat counterpart, the produced wing has an increased flexural stiffness and reduced tensile stiffness. The incorporation of chordwise unidirectional wrinkles allows fine tuning of stiffness and was experimentally found to produce 20% greater aerodynamic lift in a tethered flapping test.

(b) Wing fabrication

As mentioned, the aerodynamic performance of flapping wings is essentially determined by relevant physical properties such as density and flexural stiffness. This subsequently influences material choices and the compatible wing fabrication process. In bird-sized flapping-wing robots, researchers are less restricted on the materials and manufacturing methods. Carbon rods are the most prevalent option for constructing structural components due to its favourable stiffness-to-weight ratio [102,108–111]. Metal sheets, latex, PVC film and nylon have been experimentally employed as wing membrane [111,112]. At bird scale, artificial wings are typically constructed via a traditional simple cut-and-glue method. That is, the wingframes are bonded to the membrane using epoxy or cyanoacrylate adhesive [102,111].

The cut-and-glue approach benefits from simplicity and affordability. As the size scale reduces, the polyester film, Mylar, becomes a popular membrane material owing to its strength [105,108,110,113]. In the meantime, precision in the manufacturing process becomes increasingly important to obtain reliable results. In many cases, simple alignment mechanisms are incorporated into the assembly process to improve accuracy and repeatability of the fabricated wings [99,109,110].

A paper mould was introduced in [110] for bonding carbon rods to 15- μm Mylar film in the fabrication of a flight-capable flapping-wing device with a wingspan of 22 cm. In the fabrication process of 14 g device with 28 cm wingspan, DelFly II, a CNC machine, was used to mill the wing contours into a wooden plate. When placed on a vacuum table, the Mylar is sucked onto the plate, enabling the carbon leading edges and stiffeners to be glued using cyanoacrylate adhesive at high precision [103,113].

For wing fabrication for insect-sized devices, researchers need to overcome miniaturization challenges since conventional macroscale fabrication methods do not provide adequate precision and repeatability, while other conventional technologies for silicon-based microelectromechanical systems (MEMS) are traditionally for manufacturing devices at smaller size scales [88,105]. As a result, the MEMS-based wing fabrication technique was pioneered by Pornsin-sirirak *et al.* for a palm-sized Microbat robot that demonstrated successful free flight [88,95]. In the corresponding

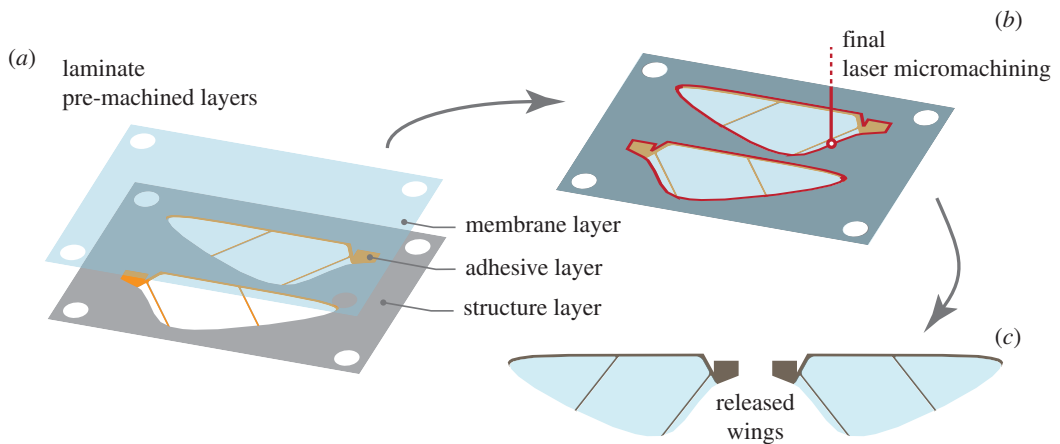


Figure 6. Schematic illustration of the wing fabrication using MEMS-based SCM process for centimetre-scale robotic wings in [97,105]. The process composed of (a) lamination of pre-machined layers, (b) singulation and (c) release.

work, the authors developed a process that enables fabrication of various model wings (for instance, beetle wings, dragonfly wings and bat wings from titanium alloy frame and parylene-C membrane). The process involves etching away titanium alloy substrate to form the wingframes and depositing Parylene-C polymers as the membrane [88].

At insect scale, another MEMS-based technique for wing fabrication was developed with techniques borrowed from the *Smart Composite Microstructures* (SCM) process [114]. In this example, 1.6 cm wings composed of carbon fibre veins and Mylar membrane were fabricated by laser-micromachining and laminating multiple material layers together using acrylic adhesives in a monolithic, planar fashion (figure 6). The technique enables features as small as $5\ \mu\text{m}$ [115]. The results were sufficiently precise and repeatable to enable the 80 mg robot to demonstrate an unconstrained flight [105]. A similar procedure was also used to construct slightly larger wings from $400\ \mu\text{m}$ thick titanium shim and $1.5\ \mu\text{m}$ Mylar film for a 3 g MAV [116,117]. To summarize the methods and materials used for fabrication of artificial wings over different scales, we tabulate an extensive list of fabricated artificial wings together with the corresponding fabrication methods and materials in table 2.

(c) Scaling laws of aeroelastic dynamics

Three-dimensionless parameters (table 3) arise when a flexible structure is considered in a flapping-wing system. The density ratio (ρ^*) describes the ratio between the equivalent structural density and fluid density. The product of the density ratio ρ^* and thickness ratio h_s^* is also called a mass ratio [7] and denotes the importance of the wing inertia relative to fluid inertia. The thickness ratio is the thickness of the wing h_s normalized by the wing chord c_m . The thickness ratio affects both the inertia of the wing and the elastic restoring force. The frequency ratio (f/f_1) is the ratio between the elastic time scale based on the first natural frequency of the wing structure $1/f_1$ and the motion time scale $1/f$. When the frequency ratio is small, the wing motion is more dominant than the structural flexibility effects and the wing can be considered as a rigid wing. Assuming that the geometric similarity is maintained, the dimensionless parameters rigid (table 1) and flexible flapping-wing aerodynamics (table 3).

It is established that shape adaptation associated with flexibility can affect the effective AoA and hence the aerodynamic outcome [74]. Wing flexibility can enhance propulsive force generation, while reducing the power consumption (e.g. [9,123–126]). Also, optimal efficiency are observed for an effective Strouhal number based on the deformed wing motion between 0.25 and 0.35 [127], similar to pitching and plunging rigid wings [15].

Table 2. Summary of artificial wings, including fabrication materials and methods.

authors	model	wing model	fabrication method	materials	
				veins	membrane
Bontemps <i>et al.</i> [118]		3.0 cm	MEMS-based	SU-8	Parylene-C
Tanaka and Wood [96]	hoverfly <i>Eristalis</i>	2.5 cm	micromoulding	thermosetting resin	
Ma <i>et al.</i> [105]	hoverfly <i>Eristalis</i>	3.5 cm	SCM	carbon fibre	mylar
Wood [104]	Dipteran	3.5 cm	SCM	carbon fibre	mylar
Meng <i>et al.</i> [97]	hoverfly Syrphidae	3.5 cm	MEMS-based	SU-8	polyimide
Campolo and Azhar <i>et al.</i> [119,120]	Dipteran	5.0 cm	chemical vapour deposition and moulding	carbon fibre	cellulose acetate film
Roll <i>et al.</i> [121]		9.0–14.0 cm	cut-and-glue	carbon fibre	mylar
Tanaka <i>et al.</i> [99]	hummingbird	12 cm		carbon fibre-reinforced plastic	Parylene-C
Pornsin-Sirirak [95]	bat	15 cm	MEMS-based	titanium alloy with carbon fibre reinforcement	Parylene-C
Ho <i>et al.</i> [106]	Cicada	15 cm	MEMS-based	titanium alloy with carbon fibre reinforcement	Parylene-C
Keennon <i>et al.</i> [122]	hummingbird	16.5 cm		carbon fibre	
Watman and Furukawa [108]		20 cm		carbon pultrusions	mylar
Sahai <i>et al.</i> [116,117]		20 cm	SCM	titanium with carbon fibre reinforcement	ultra polyester film
Nguyen <i>et al.</i> [110]	insects	22 cm	cut-and-glue with paper mould	carbon rods	mylar
Groen <i>et al.</i> and Lentink <i>et al.</i> [103,113]	dragonfly	28 cm	cut-and-glue with CNC-milled mould	carbon rods	mylar
Kim <i>et al.</i> [111]		54 cm	cut-and-glue	graphite/epoxy composite	flexible PVC

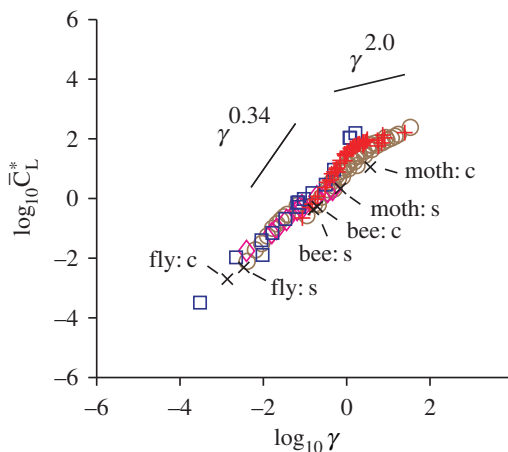


Figure 7. Scaling relationship the normalized time-averaged lift coefficient \bar{C}_L^* and γ [74].

Table 3. Dimensionless parameters in a flapping-wing system for flexible wings in addition to the parameters listed in table 1.

dimensionless parameter	symbol	definition
density ratio	ρ^*	ρ_s/ρ_f
thickness ratio	h_s^*	h_s/c_m
frequency ratio	f/f_1	f/f_1

However, our understanding of fluid physics and the resulting structural dynamics has been insufficient to explain all the salient features of the coupled fluid–structure interaction of the flapping-wing system. The main challenge is that the wing shape and motion are *a priori* unknown and complex as the unsteady aerodynamics and structural dynamics are coupled and a satisfactory analysis needs to take both effects into account together. The instantaneous shape and the rates of shape change affect the force generation and vice versa.

Scaling analyses have been successfully developed to account for the lift generation on a flexible wing (e.g. [9,124]) by capturing the first-order, important mechanism in the fluid–structure interaction. These relationships provide time-averaged estimates for the lift, power input and efficiency [9,124,127] (figure 7), consistent with relationships based on experiments [124,127]. In general, the fluid dynamic force acting on a moving wing can be decomposed into two terms: (i) the acceleration-reaction force, often linearized by the added mass [128], and (ii) the force induced by the vorticity in the flow field [9,129], or the aerodynamic damping term. For example, the rigid wing models by Theodorsen [67] forward flight and Dickinson *et al.* [26] for hover flight also include both forces. For fast flapping motions, the wing acceleration and hence the acceleration-reaction forces are greater than the vorticity-induced force [9]. Under these circumstances, the fluid dynamic force can be approximated by the added mass and scaling relationships can be established for time-averaged aerodynamic quantities [9,124,130]. For example, the time-averaged lift coefficient depends on a dimensionless shape parameter γ as

$$\gamma = \frac{\pi^2 St(1 + (4/\pi)\rho^*h_s^*)}{\rho^*h_s^*k\{(f_1/f)^2 - 1\}},$$

which is a combination of the dimensionless parameters introduced in tables 1 and 3 [9,74]. Then the time-averaged lift coefficient \bar{C}_L correlate to γ as

$$\frac{\bar{C}_L}{kh_s^*(f_1/f)^2\{1 - (f/f_1)\}} \sim \gamma^a,$$

where a decreases from 2.0 for $\gamma < 1$ to 0.34 for $\gamma > 2$ [74] as shown in figure 7.

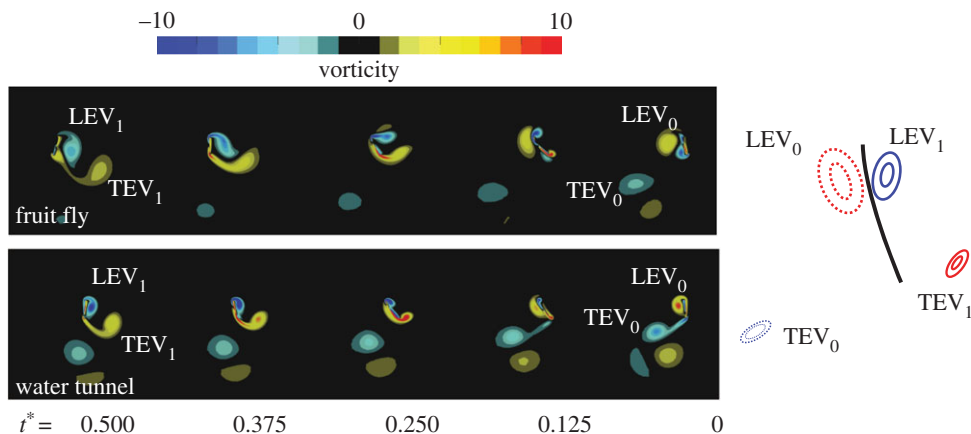


Figure 8. (Left) Vorticity contours for the optimal efficiency motion at (top) fruit fly and (bottom) water tunnel scales. (Right) Key vortex features are illustrated. Vortices indicated by dashed lines have smaller vorticity magnitudes than those with solid lines. Positive vorticity indicates counterclockwise rotating fluid elements. Negative vorticity implies clockwise rotation. Adapted from [132].

(d) Effects of wing flexibility on the flapping-wing kinematics

A fruit fly is known to enhance its lift by generating a prolonged LEV [26]. These vortical structures can often interact with the wing in the subsequent stroke, enhancing the local momentum and lift [26,29,32,74,131]. Figure 8 shows the vortical structures around a flexible flapping wing in hover at fruit fly scale that resulted in the optimal efficiency among motions with various elastic modulus of the wing and flapping amplitude [132]. A sinusoidal translation was prescribed at the leading edge. Wing rotation is purely passive due to the dynamic balance between the wing inertia, elastic restoring force and resulting aerodynamic force. A well-defined vortex LEV_0 , shed in the previous stroke, interacts with the wing at the beginning of the backward stroke [26,32,74]. A similar vortical evolution is observed at the water tunnel scale with a much lower density ratio in the bottom row of figure 8 for the optimal efficiency motion, suggesting that such wing interaction with a well-defined LEV may enhance lift without suffering too much on the power consumption. In the meantime, a new LEV_1 in the clockwise direction is generated, which reaches its maximum vorticity at around the mid-stroke and eventually sheds away from the wing.

Flapping motion of a fruit fly (*Drosophila*) is characterized by a large-amplitude, low-frequency stroke [133]. For a rigid, dynamically scaled robot, such motion is more aerodynamically efficient than a short-amplitude, high-frequency motion of a honeybee [86,133]. An ecological explanation was that bees consume floral nectar, providing a high-energy source to carry much heavier loads [133]. These studies were based on measured wing kinematics of hovering fruit flies and bees and quasi-steady models [85]. Figure 9 shows a comparison of the reported lift on a dynamically scaled, rigid fruit fly wing [85] and the resulting lift for the optimal efficiency motion that corresponds to the vorticity contours in figure 8. Overall time history of the lift and the timing of the lift peaks agree with the experimental observation. The reduced frequency and the frequency ratio for the optimal efficiency motion are $k = 0.3$ and $f/f_1 = 0.35$. The aforementioned fruit fly parameters with mean wing tip velocity correspond to $k = 0.2$, which is close to the optimal efficiency motion. The flexural chordwise stiffness of a fruit fly wing has not been determined yet, but for dragonflies the operating frequency ratio is estimated to be between 0.16 and 0.46 [134,135]. The qualitative agreement suggests that the structural properties and kinematics of the fruit fly wing may be optimized for an efficient passive wing rotation for an optimal flight.

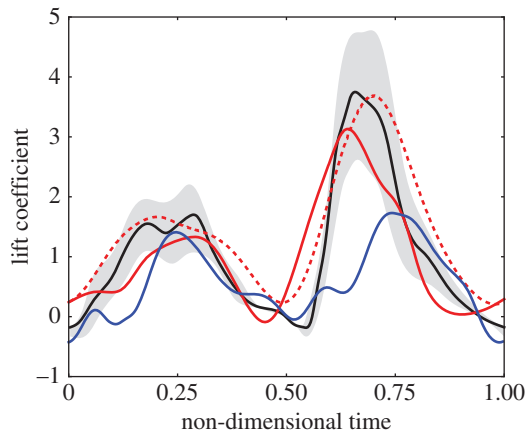


Figure 9. Comparison of time history of lift for the optimal efficient motion at (red line) fruit fly scale with (black line) experimental data [24], (blue line) three-dimensional rigid wing computational data for fruit fly [52] and (red dashed line) water tunnel scale [22]. The band around the experimental curve indicates the upper and the lower bounds. Adapted from [132].

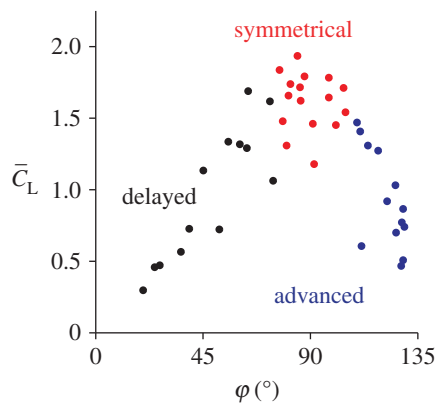


Figure 10. Time-averaged lift coefficient \bar{C}_L as a function of phase difference ϕ for a flexible flapping wing in hover. Adapted from [74].

It is well established that a flapping wing can experience a lift enhancement by controlling the phase difference between the flapping motion and wing rotation [26,39]. For rigid wings, the advanced rotation produced the highest lift, when combined with a mid-stroke AoA of around 45° [26,32]. For flexible wings, the phase difference ϕ correlates to the frequency ratio f/f_1 [74]. The large pressure differences that exist on actively rotating rigid wings near the trailing edge due to lift-enhancing rotational effects [39] are relaxed by the compliant nature of flexible wings [74]. Instead of generating rotational forces, the wing streamlines its shape such that the wing shape and motion are in equilibrium with the fluid forces, similar to the drag-reducing reconfiguration of flexible bodies [74,136]. Figure 10 shows the time-averaged lift coefficient \bar{C}_L on a passively rotating flexible wings in hover [74] at $Re = 100$ and $\rho^* = 7.8$. Young's modulus and flapping amplitude were varied to assess the aerodynamic performance of flexible flapping wings. The highest lift was obtained when passive pitch was symmetric with the imposed flapping motion with a passive pitch amplitude around 45° to 50° , showing a different qualitative trend compared to a rigid wing.

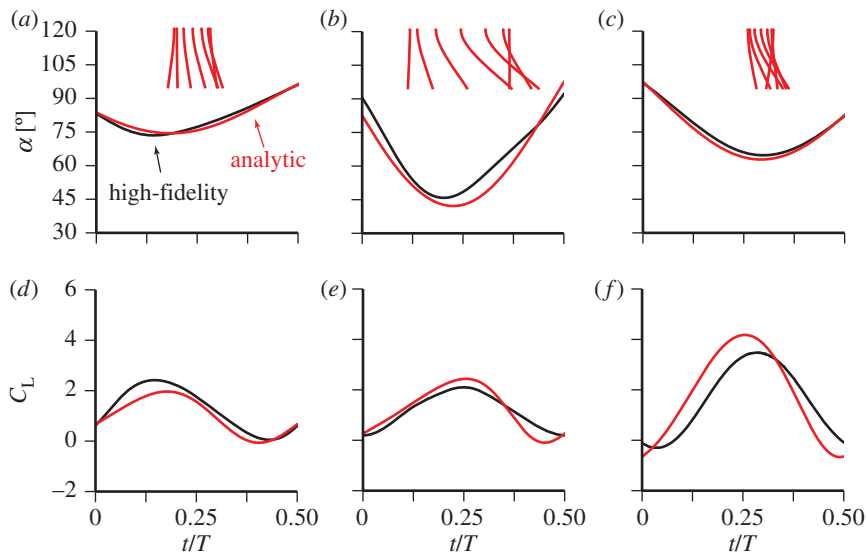


Figure 11. (a–f) Passive pitch α and lift coefficient C_L on a flexible flapping wing in hover with various timing of passive wing rotation. Red lines, analytic model with Morison equation [73]; black lines, high-fidelity computations with Navier–Stokes equations [74]. Adapted from [73].

(e) A quasi-steady model of flexible flapping-wing aerodynamics

The instantaneous information of both wing deformation and lift can be critical for the understanding of biological flight, especially in regard to offering input to flight stability and control. The dynamic flight stability is an inherent property of a flapping insect [137] with stabilization, manoeuvre and steady-state control requiring the instantaneous information about the unsteady aerodynamics and time-varying body and wing motions [137].

Under the assumption of small wing deformations, the combined fluid–structure coupling simplifies to a dynamic balance between chordwise wing deformation and drag [73]. The unsteady aerodynamic force can be modelled with the Morison equation [138] that accounts for both added mass and aerodynamic damping. Wing deformations produce a passive pitch with an AoA α , a key aerodynamic metric [74], which directly influences the generation of aerodynamic force. Specifically, the instantaneous lift follows from the quasi-steady model [26,74] based on the corresponding AoA due to wing deformations.

Figure 11 depicts the outcome of the quasi-steady model for flexible wings with the angles of attack due to passive pitch α and lift coefficients C_L as a function of time [73]. Both α and C_L agree well with high-fidelity numerical results [74]. Analysis of the contribution of the added mass and vorticity-induced forces on the resulting wing deformation suggests that the aerodynamic damping is important for an accurate prediction of phase lag of passive pitch as both forces work in opposite directions at stroke ends [73].

(f) Effects of anisotropic wing structures

Insect wings are mainly supported by wing veins and membrane. The complex arrangement of the veins and the difference of bending stiffness between the veins and membrane result in a highly anisotropic structural property [81] (figure 12). Because of the compliant nature of flexible wing, the LEV is able to grow and sustain its low pressure core on the suction side of the wing, leading to a higher lift compared with its rigid counterpart as illustrated in figure 13 [139]. Also, the timing of the passive rotation of flexible wing is determined by the structural properties in the chordwise, spanwise and torsional directions. Appropriate combination can lead to a relative

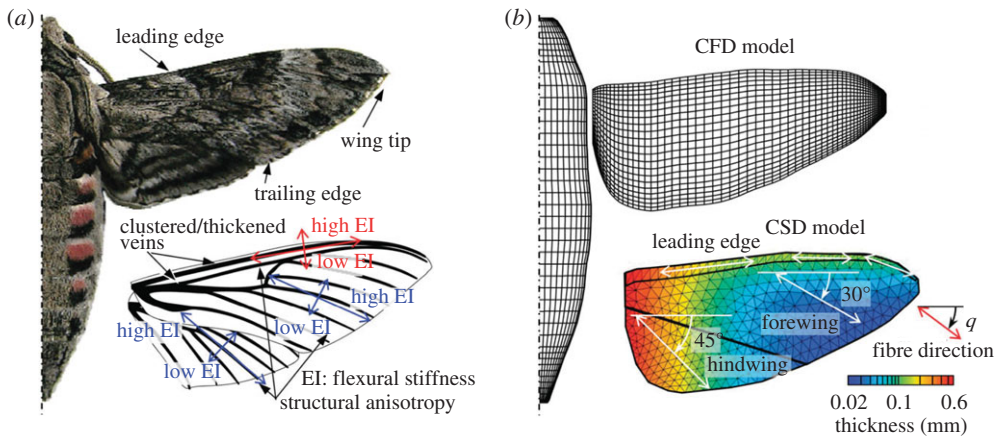


Figure 12. (a) A hawkmoth *Agrius convolvuli* with complex wing venation. (b) A computational model of the anisotropic hawkmoth wing structure. Adapted from [139].

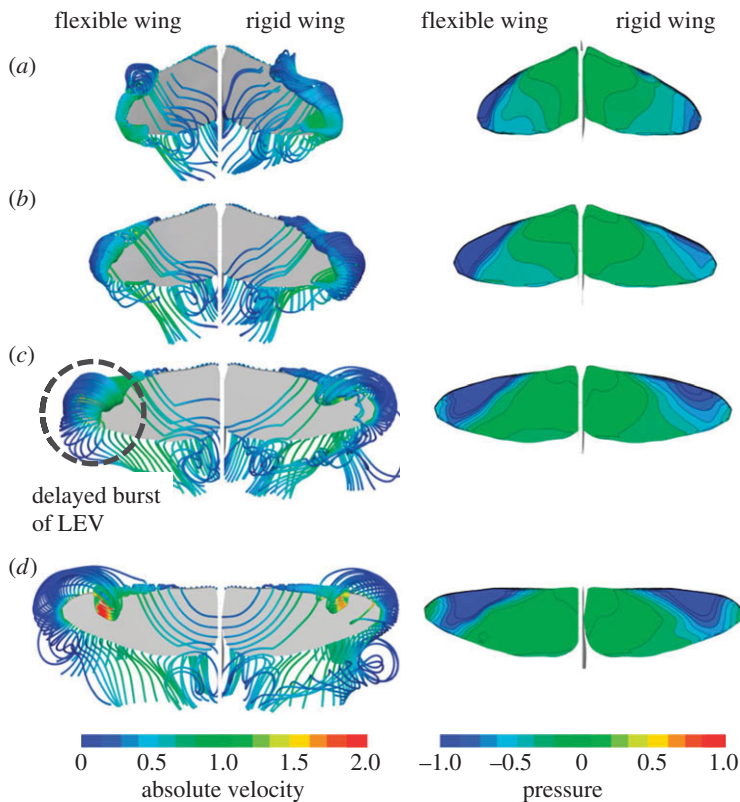


Figure 13. Streamlines and pressure contours on the flexible (left) and rigid (right) wing surfaces, illustrating the effects of wing flexibility. Adapted from [139].

phase advance of the wing rotation, which can strengthen the vortex ring and the associated downwash [26]. Overall, the wing motion is significantly affected by the spanwise bending and torsional twist [139].

Recent experiment on the fruit fly dynamics suggests that fruit fly muscles may affect the structural properties, such as the damping and elastic modulus, to modulate the wing-pitch

motion [76]. The wing deformation can also lead to a rapid stroke reversal, which can lead to greater force magnitudes [139,140]. Despite the recent efforts, the aeroelastic function of anisotropic wing structures is not fully understood due to its complexity. In addition to the direction-dependent structural properties, the wing thickness reduces significantly from wing root to tip [1,81,139,141]. The region near the wing tip passively deforms in a favourable way, whereas the wing base is ineffective for aerodynamic force generation due to the relatively lower motion velocity. As a result, an optimal dynamic spanwise distribution of the wing structure and kinematics can be a key part in achieving higher aerodynamic performance in insect flight [1].

5. Natural environment around flapping wings

The Earth's surface is highly heterogeneous consisting of natural and artificial features at all scales—from hills and cities to trees, buildings, posts, etc. Gusts, large fluctuations in wind over short durations, are also common near objects due to the transient interaction with the wind. Over the last few centuries, meteorologists have also made detailed measurements of wind properties at different altitudes and terrain but these were taken at low sampling frequencies and over long durations [142]. Aerial locomotion within the boundary layer of the Earth poses conflicting demands—crafts need to remain stable in unsteady winds yet manoeuvrable to avoid obstacles thus directly challenging the stability–manoeuvrability trade-off. Flight through such environments can be daunting as it places high demands on the sensorimotor system. The velocity changes in the freestream, due to gusts or turbulence, may affect a small vehicle considerably since the magnitude of such disturbances can be of the same order as freestream velocity. In such situations, flexible wing structures are often necessary such that the camber is adjusted in accordance with the fluctuation in flow environment. In particular, such passive control of the wing surface can better handle undesirable features such as flow separation and enhance lift-to-drag ratio. With rapid advancement in MEMs technology—sensory systems are becoming smaller and efficient [143]. A number of solutions have been adopted for flight control and path determination including biologically inspired optic flow sensors and inertial systems for flight stabilization [144,145]. Subsequent to detection MAVs rely upon motor system to perform evasive manoeuvres. This section of the review will focus on the issues and challenges on aerodynamics and flight mechanics of MAVs in natural environments.

Shyy *et al.* [66,146,147] have studied the influence of a single membrane on the *lift-to-drag ratio*, L/D , compared to a rigid aerofoil with the same nominal camber at 6% in a fluctuating freestream. It was concluded that structural flexibility can offer desirable outcome helping improve the aerodynamic performance with reduced sensitivity to fluctuations in flow environment.

Perhaps the first attempts at resolving the influence of wind unsteadiness on an unsteadily moving wing was conducted by von Karman & Sears [68] where they theoretically estimated the influence of a gust on an oscillating aerofoil. Since then a few studies have attempted to quantify the fluid mechanic interactions occurring between flapping wings and discreet aerial disturbances [148–151]. They generally observed that the aerodynamic forces recovered within a few wingbeats after advection of the gust. Lian [149] considered several cases different combinations of kinematic parameters and different ratios of gust frequency to flapping frequency. It was found that not all cases resulted in gust suppression and that no single kinematic parameter could determine the wings capability to suppress gusts. Fisher [152] quantified the performance of flapping wings by taking surface pressure measurements on a flapping flat plate subjected to different levels of turbulence. At lower reduced frequencies ($k < 0.3$), freestream turbulence directly modulated the LEV, causing large fluctuations in phase-averaged lift. However, as the reduced frequency increased, freestream turbulence had a diminishing effect on the LEV, which was attributed to the increased relative velocity of the wing with respect to the mean flow [152].

Several recent studies have considered the effect of unsteady flow environment on flapping-wing performance of wild orchid bees, bumblebees, hawkmoths, hummingbirds, etc. [106,153–159]. As expected, the unsteady flow environments result in notable impacts on flyers' flapping characteristics in order to maintain the lift, thrust and stability. In this context, it is worth

noting that, as previously summarized in §1, as a flyer's size is reduced, its flapping frequency increases. For insects, the flapping time scales are substantially shorter than those of the entire flyer. Hence, the flyer adjusts body shape, orientation and inclination over many flapping cycles. In reality, the time scales of, e.g., wind gusts, around a hertz or so, are much slower than flapping wing times. Consequently, the effect of the external flow environment is essentially quasi-steady from the view-point of flapping-wing dynamics, and the vehicle's stability and responses, while complicated by the flapping patterns, do not have to be treated in a truly unsteady flow context. Variations in winds occurring at time scales many times of the wingbeat rate are likely to have a limited effect on flight control since they may be treated as quasi-steady changes in ambient conditions. For flyers such as bats and birds, the flapping time scale and the body's time scale are closer and the impact of the unsteady flow environment needs to be addressed in a continuous time-dependent framework.

The response to wind-induced disturbances can either be active, passive or a combination of the two. Active response will include modulation of wing kinematics in response to forces and torques induced by the wind [153,158,160–162]. Moreover, changing body posture to increase flight stability has been observed [156]. Other animals such as mosquitoes have devised passive strategies to deal with similar conditions. Other mechanisms including flapping counter torque [163,164] and dihedral stability [165] and unconventional mechanisms such as vibrational stabilization [166] further augment flight stability of flapping wings to aerial disturbance.

Flight in cluttered environment places adds demands on the motor system since it needs to not only produce the force necessary for weight support but also to perform aerial manoeuvres. To produce additional power flappers can either increase the flapping frequency, amplitude or feathering angle (or a combination of the three). The control of feathering angle in insects and in some birds is still relatively unknown with supporting evidence present for both active and purely passive control. Miniature robotic flapping-winged flyers have generally opted for passive wing feathering as a means of reducing the control variables without sacrificing on aerodynamic performance [105,167]. Few investigations have also assessed the optimum control mechanisms for insect-scale flyers [168] and explored design alternatives that adopt a minimal actuation approach [169]. Dimensionally, both amplitude and frequency have similar influence on force production [170]; however, insects such as honeybees and bumblebees tested using load-lifting paradigms or in a rarified fluid medium reveal that they generally increase stroke amplitude to increase aerodynamic force [133,160,171]. Other flyers such as hummingbirds can vary flapping frequency [158,172] as well. Increasing amplitude will likely increase the force produced at mid-stroke [27], whereas increasing flapping frequency will increase the role of other phenomena such as wake recapture, rotational lift [26] or passive pitch due to wing flexibility [9,74].

The trade-off between stability and manoeuvrability is considered axiomatic. However, flapping-winged flyers have the potential to maintain both mutually opposing properties. Recent research on the dynamics of fish shows that the production of antagonistic forces increase manoeuvrability without sacrificing stability [173]. Similarly, the wing of insects and birds produce large instantaneous forces while flapping that are not always along the direction of mean displacement yet they continue to maintain equilibrium since these forces are cancelled by equal and opposite forces produced by the contralateral wing. Modulation of these forces through bilateral asymmetry can produce torques that can be used for performing corrective manoeuvres in unsteady winds or to take evasive flight when nearing obstacles [165]. Additionally, flapping wings have been shown to be more resistant to gusts and freestream turbulence [149,152].

6. Roles of sensor in flight control and stability

In the absence of inherent flight stability as found in flying insects [174,175] or some flapping-wing robotic systems [105,122], an active control feedback system is essential. Flying insects rely on the provision of rich sensory feedback across a wide range of modalities. Inputs from across multiple

sensors such as compound eyes, ocelli and antennae are combined and used as feedback to the flight control system at different levels. In artificial flying machines, the equivalent data fusion process is also required to amalgamate visual information and data from sensors into functional forms for state feedback [176,177]. In this section, we explore fundamental characteristics of both biological and man-made sensors and their roles in flight stability and control.

(a) Inertial sensors

Inertial sensors have become a critical component of MAV flight control system as they provide vital information required for attitude stabilization [176,177]. Flying insects equipped with such sensors are under various forms. Halteres of dipteran flies are best known to function under the same principle as a vibratory gyroscope. It is believed that antennae of some insects might play an analogous role to halteres. While inertial data such as rotational and translational rate can be deduced from visual information, they often suffer from sensorimotor delay associated with phototransduction and motion computation in contrast to minimal latency from the aforementioned mechanosensory organs. Given the swift dynamics of small flying insects, the visual feedback delay (estimated to be 50–100 ms or 10–20 wing strokes in fruit flies) can lead to instability as it often exceeds the tolerable latency as predicted by the linear system theories [92].

(i) Halteres

While many flying insects possess two pairs of wings, in houseflies and their relatives the dipteran insects, their hind pair has been modified into mechanosensory organs known as halteres. These club-shaped structures, oscillating up and down at wingbeat frequency, are believed to be sensitive to Coriolis forces during aerial manoeuvres for measurement of body angular velocities [178]. It is thought that the mechasensory reflex from halteres is crucial for attitude stabilization in dipteran flies [179]. It was reported that removal of halteres radically changes the behaviour of *Calliphora*, causing them to crash immediately when thrown into the air [180]. Similarly, Ristroph *et al.* showed that haltere-disabled fruit flies were unable to maintain stable flight [92].

Based on the dynamics of flies or insect-scale flapping-wing robots, theoretical frameworks suggest that rotational rate feedback alone is sufficient for attitude stabilization [181,182]. While rotational rate feedback may also be obtained from processing visual information, it may not be adequate when the sensorimotor delay of feedback is taken into account. Using linear system theories, Ristroph *et al.* [92] estimated values of tolerable latency or reaction time of the sensory-motor flight control systems of various insects. The theoretical value of tolerable reaction time of fruit fly is 13 ms—far below the latency of the visual system (≈ 50 ms), but notably longer than the haltere response found in [183]. The study explains why visual feedback alone is insufficient for flight stability, whereas the low latency of haltere feedback enables hard-wired equilibrium reflexes for attitude stability in dipteran insects.

The absence of halteres in other flying insects could be partially explained by the presence of other sensors playing similar roles. For instance, vibrating antennae in hawkmoths was found to hold a similar role of mediating flight stability during manoeuvres [184,185]. The antennal vibrations are transduced in a frequency range characteristic to the Coriolis input. As a result, removal of the antennal flagellum acutely disrupted flight stability in moths [184]. In addition to halteres and antenna, it is also known that most flying insects carry simple light sensors known as ocelli that might allow them to rapidly perform self-righting manoeuvres. However, it is still unverified how other insects such as honeybees accomplish attitude stabilization [182].

(ii) Ocelli

Adult insects typically possess two compound eyes and three ocelli [186]. These ocelli, or rudimentary defocused light sensors, are situated dorsally to view the entire upper hemisphere. While their precise role in flight stabilization is not completely understood [187], it is believed that ocelli may function synergistically with the compound eyes to minimize the delay of visual

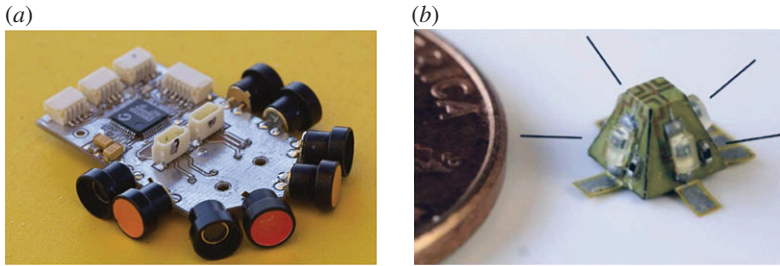


Figure 14. (a) An ocelli mimicking device consisted of eight photodiodes. The sensor identifies the horizon based on the polarization of the sky. Adapted from [190]. (b) A 25 mg ocelli-inspired sensor with four phototransistors arranged in a pyramid shape. Adapted from [182].

responses [188]. A head rotation would shift the position of the ocelli with respect to the sky and the ground, altering the optical simulations received by different ocelli, which can be used to sense attitude deviation [189]. Signals from three ocelli appropriately located allow the robust estimation of roll and pitch.

In robotic systems, the concept of horizon sensing has been investigated. A number of low power ocelli-inspired sensors and associated models have been engineered. Examples include a 6 g miniaturized navigation sensor shown in figure 14 [190,191], inertial measurement unit (IMU)-integrated ocelli sensors for MAVs [109] and a 25 mg artificial ocelli consisting of four phototransistors [182] (figure 14). In [182], the signals from the ocelli-inspired sensor were processed to obtain angular velocity feedback (instead of attitude) and used to stabilize the insect-scale robot in short take-off flights [182].

(iii) Inertial measurement units

MEMS IMUs have become a standard onboard sensing device in unmanned aerial vehicles and many robotic systems. An IMU is typically equipped with a 3-axis accelerometer, a 3-axis gyroscope and sometimes a magnetometer or a GPS receiver. Linear accelerometers on IMUs measure non-gravitational accelerations of the vehicles [177]. As a consequence, IMUs are unable to directly provide attitude feedback for flying vehicles. Interestingly, this characteristic parallels the finding that there is no indication that insects use a static sense of gravity in flight [180]. In engineering communities, estimation or filtering algorithms are employed to obtain the estimate of the vehicle's attitude from the accelerometer's and gyroscope's readings [177,192].

In contrast to the accelerometer measurements, angular velocity information from the gyroscope could be directly used for attitude stabilization in a similar fashion to halteres in Diptera [122,193]. However, it has been shown that in some flapping-wing vehicles, angular velocity measurements from MEMS gyroscopes on flapping-wing vehicles with two wings potentially suffer from inherent oscillation about the pitch axis (flapping-wing devices with X-wing configuration as in [103,194] could be less susceptible to this vibration) [122,193]. Thus far, the use of IMUs on flapping-wing systems has been limited as many developed prototypes possess passive stability [103,194]. The use of IMU readings for attitude stabilization in unstable flapping-wing vehicles remains a largely unexplored research topic.

(iv) Antennae

Almost all insects possess a pair of antennae which serves different functions in mechanoreception, chemoreception, etc. [195]. The antennae of jewel beetles can detect substances emitted in smoke from burning wood [196]. Sensory neurons found in the antennal flagellum of the moth *Manduca sexta* play a crucial role in maintaining flight stability [184]. Another role of insect antennae in flight control as air-current sensing organs in many insects is mentioned in [197–199]. Experiments suggested that flies tend to maintain constant groundspeed despite

changes in wind speed, implicating the presence of an active feedback regulator [200]. It is speculated that incident wind causes the deflection of arista. The deflection, which superimposes upon the small antennal oscillations at wingbeat frequency, is then detected by the stretch-sensitive scolopial receptor called the Johnston Organ on the flagellum [188]. While vision can also provide flight speed feedback, its long latency may have adverse effects. Fuller *et al.* [201] demonstrated that *Drosophila* rely on short delay response (approx. 20 ms) from antennae to augment the visual response that has the sensorimotor delay of 50–100 ms to actively regulate flight speed, resulting in a multi-model sensory feedback architecture. Without fast feedback from the antennae, the feedback loop with high gain is susceptible to instability.

Small flapping-wing robots operating in outdoor environments are susceptible to wind disturbances [160]. The effects from damping force and torque are amplified by the flapping motion of the wings [92,201]. Combined with inherent instability, fast corrective feedback is likely to be crucial to maintain attitude stability. Small MEMS-based air sensors have been proposed [202–204]; nevertheless, they have yet to be implemented and tested on flapping-wing vehicles.

(b) Visual sensing

Various flight behaviours in flapping-wing insects and birds are tightly linked to visual sensing. Vision is critical to navigation [189], landing [205], chasing prey, avoiding obstacles, as well as stabilizing flight [206]. Unlike larger animals that mostly use stereopsis and object recognition to navigate and estimate distance, tiny insects rely on compound eyes. Consisting of numerous simple facets, compound eyes are very sensitive to motion [189]. Accordingly, insects rely on calculations of optic flow, which provide a measure of the ratio of velocity to distance, to process directional motion.

(i) Compound eyes

In arthropods, evolution has created a sophisticated imaging system known as compound eyes. A hexagonal eye lattice of the compound eyes consists of hundreds or thousands of individual photoreceptor units or ommatidia arranged on a convex surface, resulting in an extended visual field [199,207]. Panoramic vision is a prominent feature of insect visual systems. Visual cues serve multiple purposes in insect flight, for instance, goal-directed behaviour such as visually guided landing [208] and evading looming targets [209]. In most circumstances, visual information is often exploited in the form of optic flow.

(ii) Optic flow

As mentioned, insects rely heavily on vision to perceive their position and velocity relative to objects around them. While moving through a stationary environment, insects experience apparent motion of these objects as panoramic retinal image shifts, or optic flow. A formal vector notion of optic flow was introduced in [210] describing image velocities. The optic flow essentially measures the ratio of movement to the distance of surrounding objects, resulting in nearby objects appearing to move faster than distant objects. The coupled relationship renders the estimation of absolute distance or velocity from optic flow challenging. While local velocity vectors in flow fields of different motions may appear similar, they could be distinct on a global scale. Optic flow fields induced by translation are fundamentally different from those induced by rotation as illustrated in figure 15. Analysing the optic flow field allows the animal to assess its motion and use this information for control and navigation purposes.

Ample evidence suggests flying insects rely heavily on optic flow. It has been shown that bees depend on optic flow to avoid obstacles [212,213]. Several studies have confirmed that many insects directly control flight speed in the presence of wind disturbance by using optic flow information [201,214,215]. The fact that the magnitude of the optic flow field is inversely proportional to the distance enables insects to spontaneously modulate the flight speed as a function of the distance to the ground or corridor in a strategic manner (figure 16). Bees were found to perform landing manoeuvres by maintaining constant image velocities, allowing the

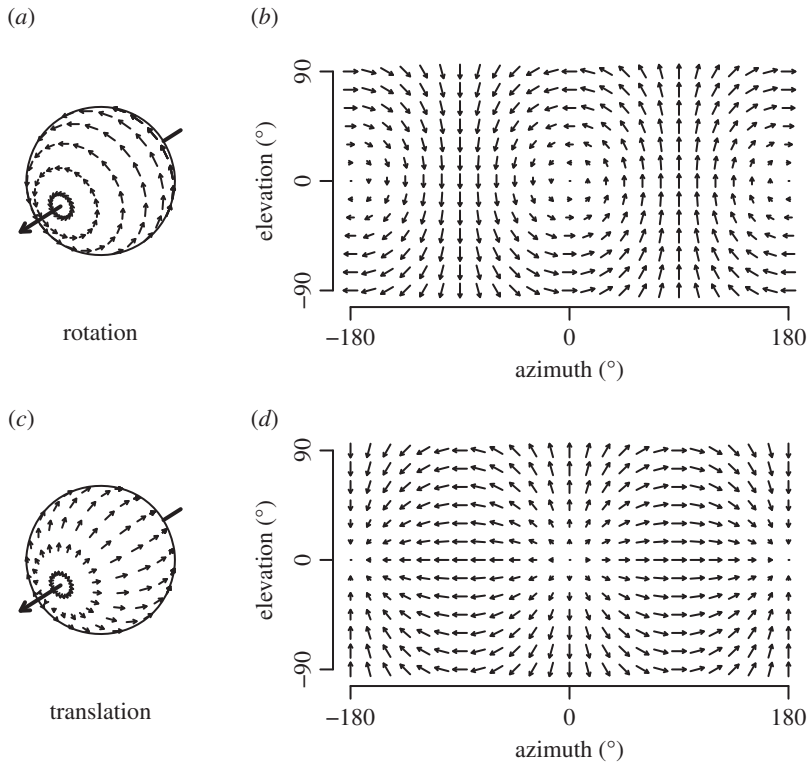


Figure 15. The optic flow experienced by an observer performing a rotation about a roll axis (*a,b*) and a translation in the frontal direction (*c,d*). Flow fields are shown in spherical coordinates (*a,c*) of the visual field (*b,d*). Adapted from [211].

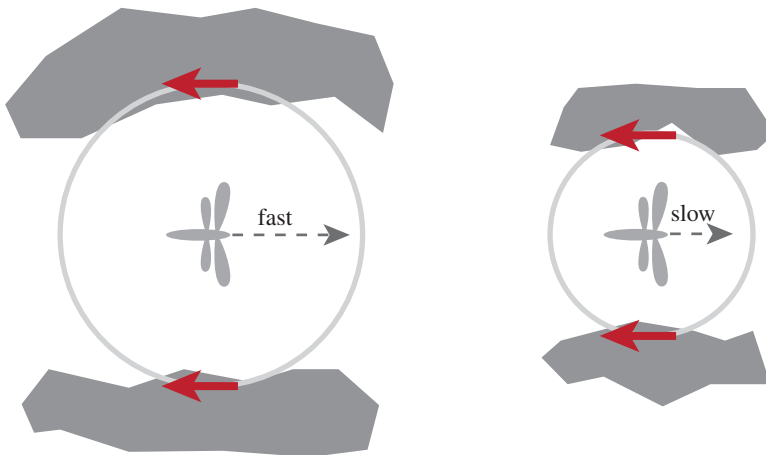


Figure 16. An insect flying through a corridor or complex obstacles can strategically modulate the flight speed by regulating the optic flow magnitude. The results in slower flight speed in more cluttered environments. In the meantime, the insect centres itself in the middle of the corridor by balancing the optic flow information from both sides.

flight speed to decrease progressively as they approach the ground [189,205]. Regulation of lateral image velocities at constant value is a simple and elegant solution that automatically reduces flight speed when negotiating a narrow passage or flying through densely cluttered environment [189,215]. The principle has been implemented on a flying rotary MAV with an omnidirectional fisheye camera for providing optic flow to safely navigate through an indoor corridor [216].

(iii) Machine vision

Traditional CMOS cameras have been equipped on centimetre-scale flapping-wing robots [122,217]. Similar to insects, vision assists flying robots to autonomously navigate and avoid collision. Advances in deep learning and object recognition potentially enable vehicles to perform various tasks such as assisted pollination, reconnaissance, or search and rescue [218].

Vision-based sensors have been successfully incorporated into flying vehicles. Particularly for navigation in a GPS-denied environment, a stereo camera and a laser range finder were equipped onboard for simultaneous localization and mapping algorithms [219,220]. The weight and computation requirements of these sensors render them suitable for large flapping-wing robots with slower dynamics such as a Robo Raven in [221].

Lightweight flapping-wing vehicles with restricted payload, however, encounter a similar limitation faced by insects. Processing visual information from traditional cameras is computationally and energetically expensive. Several researchers have turned to a biologically inspired approach to illustrate the use of low spatial resolution sensors for robot navigation similar to the use of optic flow in insects [222–224]. In [223], a 33 mg one-dimensional optic-flow-based sensor was mounted on an insect-scale robot to provide altitude feedback in a constrained flight. Curved artificial compound eyes have been developed to produce high temporal resolution and large field of view images [207,225,226] and deployed for operation of flying robots to provide optic flow cues for guidance [224].

7. Flight dynamics and control in insect flight

(a) Coupled approach and passive versus active stabilization

Natural flyers possess excellent flight control and manoeuvrability while continuously varying their wing kinematics and shapes, as well as body inclination [86,227]. Powered flight in insects requires an integrated system consisting of wings to generate aerodynamic force, sensors to assess the flight environment, muscles to move the wings and a control system to modulate power output from the muscles. Uncovering the novel mechanisms how insects control flight needs to unpick the dynamic complexity of the sensorimotor neurobiology (motor pattern, central nervous system and sensory feedback), the musculo-skeletal mechanics (skeletal system, muscle forces, and muscle physiology and anatomy) and the aerodynamics (flexible wing and body dynamics) [228].

In response to multi-modal sensory input, insects use sensorimotor pathways to modulate power output from the muscles to the wing. Consequently, a closed-loop system integrating inner workings of the sensorimotor neurobiology and musculo-skeletal mechanics and an external multiple mechanical system is established to handle aerodynamics and structural mechanics of flexible wing and body as well as flight dynamics.

Studies on insect flight stability and manoeuvrability have been conducted mostly based on experiments in terms of visually mediated response [229–231] and haltere-mediated response [179,232,233]. As discussed, compound eyes, ocelli and halteres of insects play important roles in sustaining stability and manoeuvrability. When insects respond to the external environment, the visual interneuron systems (compound eyes and ocelli) encode optical changes in flow fields such as slow forward translation, roll or pitch rotation. Motor neurons control neck and wing muscles, which receive the input information from motion-sensitive neurons in the visual system and halteres afferents, and then give corresponding responses to maintain stable flight [234]. Studies on active control of flying insects indicate that the visual and haltere systems are capable of sensing body deviation and enable insects to provide compensation reactions in maintaining equilibrium.

In order to understand how the inner control system responds to external perturbations and what kind of wing–body kinematics will be employed, the key questions regarding how the wing–body kinematics, the inertial and aerodynamic forces, and the dynamics of body attitude interact with each other need to be addressed [175,235]. An integrated multi-mechanical system

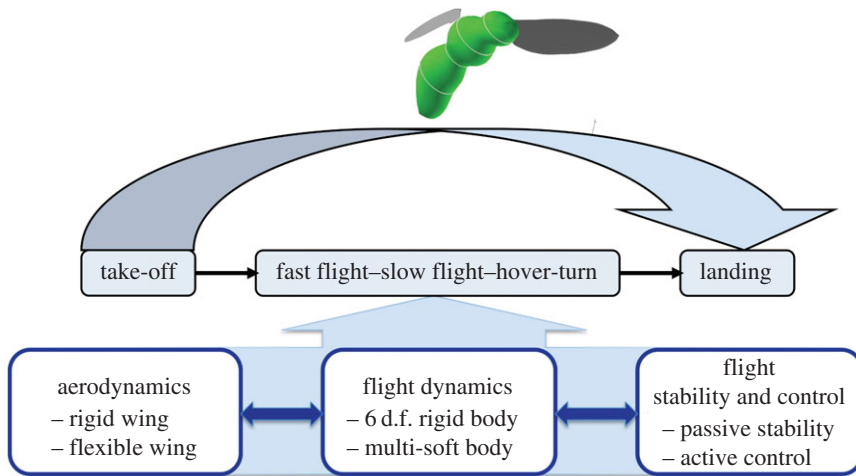


Figure 17. Diagram of bioinspired multi-mechanical systems [236].

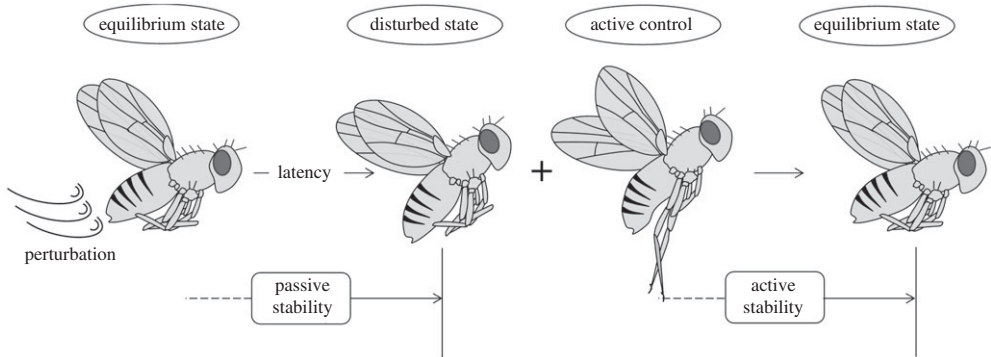


Figure 18. Schematic diagram of passive and active stability during flapping flight. During a latency period, fruit flies exhibit passive response without any active feedback control of wing and body kinematics [235].

associated with flapping wings kinematics, aerodynamics and structural mechanics of flexible wing and body as well as the 6 d.f. flight dynamics of the body is schematically shown in figure 17 [236].

Insect flight shows some latency period, defined as the time delay between sensory sensitivity neurons and motor neurons (figure 18) when experiencing sudden perturbation such as wind gust [237,238]. Any active feedback controls including head movement and wing kinematics are unavailable during the latency period and all behavioural responses occur in a passive way.

Such passive stabilizing, including unconventional mechanisms, as investigated in [164,166,239] overcome processing delays by interacting with active, sensory-based equilibrium reflexes in flying animals [179,240,241]. Taylor & Zbikowski [241] studied insect flight stability of locusts measuring directly the forces and moments of a tethered animal and averaged over stroke periods. In subsequent studies [242–245], based on time-resolved wing and body kinematics in both tethered and free-flight conditions [242,243], measurement of the aerodynamic forces and moments in response to perturbations with respect to an equilibrium flight condition, a matrix of a linearized aerodynamic system is developed to estimate the flight stability via the eigenvalue analysis. These analyses have identified at least one unstable mode, suggesting possible intrinsic flight instability of insects as well as highlighting the importance of feedback-based modulation of the wing kinematics so as to achieve stable flight.

(b) Averaged and linearized models

Most analysis of flight dynamics of miniature natural and artificial flyers has been conducted by extending methods developed for manned aircrafts [27,30,71,137,246,247]. This includes adopting the same coordinate system and similarly deriving the governing equations that mediate flight dynamics. As with fixed wing crafts, the motion is governed by the equations of motion coupled with the Navier–Stokes equations. On conducting stability analysis, albeit with the assumption of small perturbations, flapping flight has been found to be unstable [137,248–251] and thus active control is necessary to remain airborne. The instability arises from multiple eigen modes occurring over different time scales along the longitudinal and lateral directions [1,137]. Accounting for all time-resolved forces and torques produced while flapping and the subsequent body dynamics will involve direct numerical simulation of the aerodynamic forces and body dynamics including compliance, which is still challenging and requires enormous computational resources. Readers are referred to [137,174,252] for a detailed review of the current state of stability analysis of insect-scale natural and artificial flight.

A number of researchers have developed averaged linearized models of flight control that have sought to exploit that large disparity in the time scales of wingbeat frequency and motion dynamics, as discussed in §1. In these models, the flapping wings are assumed to produce a mean aerodynamic force. The simplicity and versatility of the averaged model have enabled their application in the majority of the existing studies on insect flight dynamics [240,244,247,250,253–256]. Theoretical validations and simplified direct numerical simulations reveal that averaged models are indeed suitable approximations of insect flight control [137]. Such models have also been applied to study the manoeuvring flight of hawkmoths that are relatively large and have relatively lower wingbeat frequency, yet the times scales of natural modes of motion of the body divided by the wingbeat period are relatively large [164,257]. This model has been further extended to the helicopter analogy where the (mean) aerodynamic force produced is assumed to be constant in the body coordinate system [246,254]. As per this model, translation is accomplished by reorienting the mean aerodynamic force vector to render a non-zero component in the desired direction. Therefore, translation along the longitudinal and lateral directions needs to be coupled with pitch and roll, respectively. This relatively simple model for flight control can be used to study flight manoeuvres of a number of insects and birds [154,209,258–260]. But, animals possess an extensive repertoire of kinematic variability that permits them to perform manoeuvres that deviates from the helicopter model such as translating maintaining constant body orientation (side-slipping) [261].

Taking into account the time-variant nature of flapping-wing motion by coupling the equations of 6 d.f. motion with the Navier–Stokes equations, Gao *et al.* [235] studied the flight dynamics of fruit fly hovering and found that there exists an instability that at least one state variable tends to diverge after several wingbeat cycles. This study further indicated that a fruit fly does have sufficient time to apply some active mediation to sustain steady hovering before losing body attitudes. It should be pointed out that, as demonstrated by Taha *et al.* [262], higher order averaging techniques may be needed to understand the dynamics of flapping-wing flight and to analyse its stability. Suffice it to say that direct accounts of the flexible wing structures and their coupling with the fluid dynamics and flight stability are still lacking in the literature.

Using a dynamically scaled robotic model, Elzinga *et al.* [263] studied the longitudinal flight dynamics for flies at various levels of forward flight and suggested that the steady-state lift and thrust requirements at different speeds may be accomplished with quite subtle changes in hovering kinematics, and that these adjustments act primarily by altering and achieving the pitch damping to ensure stability. Such a control scheme would provide an elegant solution for stabilization across a wide range of forward flight speeds. The question of how insects regulate and stabilize flight via changes in wing activation and body kinematics is an open and actively researched area [242,264–266].

With the increasing number of artificial flapping-wing systems [95,97,105,116,121,122], researchers and engineers have explored beyond the linear control methods proposed by

biological studies [253,263,264] and have employed techniques borrowed from the MAV community for controlling both wing trajectory [221,267] and flight [105,268]. Adaptive schemes have been implemented to compensate for uncertain parameters in the models to improve the tracking precision [269]. These engineering topics can be considered parallel to an ability to learn and adapt in insects and animal, which is yet still a largely unexplored research area.

8. Concluding remarks and perspective

Various aspects of biological and bioinspired flyers are reviewed. As far as the flapping-wing aerodynamics is concerned, the flow is unsteady and a quasi-steady model based on the nominal position and angles of a wing relative to undisturbed freestream does not properly account for the main physics. An adjusted quasi-steady model by correcting the surrounding flow parameters including the effective AoA and associated flow structures such as jet flows, can work much better. For larger (bird, bat) scale vehicles, since the flapping and the vehicle time scales are not separable, a time-dependent approach is needed to address the vehicle stability and control issues along with the instantaneous flapping-wing characteristics. On the other hand, for insect-scale vehicles, since the flapping time scales are much shorter than the vehicle's response time scale (figure 1), as far as the vehicle flight stability and control are concerned, averaged flapping-wing aerodynamic parameters can be used. Consequently, while the insect-scale flyers experience highly varied flight conditions, their behaviours in aerodynamics as well as flight planning, sensing and control can be cast in quasi-steady framework, taking the environmental fluctuations as time-dependent boundary conditions. However, higher order averaging techniques may be needed to understand the dynamics of flapping-wing flight and to analyse its stability. Furthermore, intrinsic interactions between flexible wing structures, flight stability and associated aerodynamics are open issues awaiting further investigation.

A low aspect ratio flapping wing also exhibits notable different behaviours compared with a fixed wing, including flow structures, much enhanced lift due to coherent vortical flow structures and related pressure effects, and spanwise variations including the possibly benign effect of tip vortices. The coordination between plunging, pitching and sweeping parameters is critical for aerodynamic performance of flapping wings. It is observed that for a rigid wing, while advanced rotation (ahead of the end of plunging) can enhance lift, for an insect-scale flyer, the wing flexibility and passive pitching introduces aerodynamic benefit resulting in symmetric rotation and plunging to be preferred.

The advancement in microscale structural and material design and fabrication now enables us to engineer insect-scale flyers. Coupled with new insight gained from sensing and control research, highly controllable flight is now realizable for insect-scale flyers.

Looking forward, there is a clear need to investigate sensorimotor neurobiology, musculo-skeletal mechanics, and flapping, flexible wing aerodynamics, stability and control in a coherent and unified framework. In contrast to conventional fixed wing aircraft design, with aerodynamic derivatives and control laws designed and developed separately, insect-scale flyers require that sensors, motors, muscles, skeletons, wings and bodies, and their combined behaviour and performance be investigated altogether. Such an integrated, bioinspired flight system will shed new light on miniaturized-scale flyers' characteristics and capabilities. There is great room for innovation in terms of developing future bioinspired flyers, benefitting from light, flexible structures and materials, new aerodynamic understanding combining with real-time sensing and control with active and passive systems, and capable of performing wide ranged missions.

Authors' contributions. All authors were involved in developing the scope and preparing the contents of the paper. All authors gave final approval for publication.

Competing interests. We have no competing interests.

Funding. We received no funding for this study.

Acknowledgements. W.S. and C.K. did much of the relevant research reported here while in Ann Arbor, MI, as well as in our current institutions. We thank the University of Michigan for providing a conducive environment, and the various agencies for supporting our endeavors.

References

1. Shyy W, Aono H, Kang C, Liu H. 2013 *An introduction to flapping wing aerodynamics*. New York, NY: Cambridge University Press.
2. Dial KP. 1994 Inside look at how birds fly: experimental studies of the inertial and external process controlling flight. In *Thirty-Eighths Symp. Proc. Experimental Test Pilots*, Lancaster, CA, USA, pp. 301–314. Lancaster, CA: Society of Experimental Test Pilots.
3. Norberg UM. 1990 *Vertebrate flight: mechanics, physiology, morphology, ecology, and evolution*. New York, NY: Springer.
4. Goslow GE, Dial KP, Jenkins FA. 1990 Bird flight: insights and complications. *Bioscience* **40**, 108–115. (doi:10.2307/1311343)
5. Shipman P. 1999 *Taking wing: archaeopteryx and the evolution of bird flight*. New York, NY: Simon and Schuster.
6. Acheson DJ. 1990 *Elementary fluid dynamics*. New York, NY: Oxford University Press.
7. Fung YC. 2008 *An introduction to the theory of aeroelasticity*. New York, NY: Dover publications, inc.
8. Barenblatt GI. 2003 *Scaling*. Cambridge, UK: Cambridge University Press.
9. Kang C, Aono H, Cesnik CES, Shyy W. 2011 Effects of flexibility on the aerodynamic performance of flapping wings. *J. Fluid Mech.* **689**, 32–74. (doi:10.1017/jfm.2011.428)
10. Shyy W, Liu H. 2007 Flapping wings and aerodynamic lift: the role of leading-edge vortices. *AIAA J.* **45**, 2817–2819. (doi:10.2514/1.33205)
11. Birch JM, Dickinson MH. 2001 Spanwise flow and the attachment of the leading-edge vortex on insect wings. *Nature* **412**, 729–733. (doi:10.1038/35089071)
12. Triantafyllou MS, Triantafyllou GS, Yue DKP. 2000 Hydrodynamics of fishlike swimming. *Annu. Rev. Fluid. Mech.* **32**, 33–53. (doi:10.1146/annurev.fluid.32.1.33)
13. Eloy C. 2012 Optimal Strouhal number for swimming animals. *J. Fluids Struct.* **30**, 205–218. (doi:10.1016/j.jfluidstruct.2012.02.008)
14. Koochesfahani MM. 1989 Vortical patterns in the wake of an oscillating airfoil. *AIAA J.* **27**, 1200–1205. (doi:10.2514/3.10246)
15. Triantafyllou GS, Triantafyllou MS, Grosenbaugh MA. 1993 Optimal thrust development in oscillating foils with application to fish propulsion. *J. Fluids Struct.* **7**, 205–224. (doi:10.1006/jfls.1993.1012)
16. Triantafyllou MS, Triantafyllou GS, Gopalkrishnan R. 1991 Wake mechanics for thrust generation in oscillating foils. *Phys. Fluids A Fluid Dyn.* **3**, 2835. (doi:10.1063/1.858173)
17. Taylor GK, Nudds RL, Thomas ARL. 2003 Flying and swimming animals cruise at a Strouhal number tuned for high power efficiency. *Nature* **425**, 707–711 (doi:10.1038/nature02000)
18. Dabiri JO. 2009 Optimal vortex formation as a unifying principle in biological propulsion. *Annu. Rev. Fluid Mech.* **41**, 17–33. (doi:10.1146/annurev.fluid.010908.165232)
19. Weis-fogh T. 1973 Quick estimates of flight fitness in hovering animals, including novel mechanisms for lift production. *J. Exp. Biol.* **59**, 169–230.
20. Lehmann F-O, Pick S. 2007 The aerodynamic benefit of wing–wing interaction depends on stroke trajectory in flapping insect wings. *J. Exp. Biol.* **210**, 1362–1377. (doi:10.1242/jeb.02746)
21. Lehmann F-O. 2009 Wing-wake interaction reduces power consumption in insect tandem wings. *J. Exp. Biol.* **46**, 765–775.
22. Cooter RJ, Baker PS. 1997 Weis-Fogh clap and fling mechanisms in *Locusta*. *Nature* **269**, 53–54. (doi:10.1038/269053a0)
23. Goëtz KG. 1987 Course-control, metabolism and wing interference during ultra-long tethered flight in *Drosophila melanogaster*. *J. Exp. Biol.* **128**, 35–46.
24. Brodsky AK. 1991 Vortex formation in the tethered flight of the peacock butterfly *Inachis io* and some aspects of insect flight evolution. *J. Exp. Biol.* **161**, 77–95.
25. Srygley RB, Thomas ALR. 2002 Unconventional lift-generating mechanisms in free-flying butterflies. *Nature* **420**, 660–664. (doi:10.1038/nature01223)
26. Dickinson MH, Lehmann F-O, Sane SP. 1999 Wing rotation and the aerodynamic basis of insect flight. *Science* **284**, 1954–1960. (doi:10.1126/science.284.5422.1954)
27. Sane SP, Dickinson MH. 2002 The aerodynamic effects of wing rotation and a revised quasi-steady model of flapping flight. *J. Exp. Biol.* **205**, 1087–1096.
28. Lehmann F-O, Sane SP, Dickinson MH. 2005 The aerodynamic effects of wing-wing interaction in flapping insect wings. *J. Exp. Biol.* **208**, 3075–3092. (doi:10.1242/jeb.01744)

29. Birch JM, Dickinson MH. 2003 The influence of wing-wake interactions on the production of aerodynamic forces in flapping flight. *J. Exp. Biol.* **206**, 2257–2272. (doi:10.1242/jeb.00381)
30. Wang ZJ. 2005 Dissecting Insect Flight. *Annu. Rev. Fluid Mech.* **37**, 183–210. (doi:10.1146/annurev.fluid.36.050802.121940)
31. Shyy W, Trizila P, Kang C, Aono H. 2009 Can tip vortices enhance lift of a flapping wing? *AIAA J.* **47**, 289–293. (doi:10.2514/1.41732)
32. Trizila P, Kang C, Aono H, Shyy W, Visbal M. 2011 Low-Reynolds-number aerodynamics of a flapping rigid flat plate. *AIAA J.* **49**, 806–823. (doi:10.2514/1.J050827)
33. Ellington CP, van den Berg C, Willmott AP, Thomas ALR. 1996 Leading-edge vortices in insect flight. *Nature* **384**, 626–630. (doi:10.1038/384626a0)
34. Berg van den C, Ellington CP. 1997 The three-dimensional leading-edge vortex of a ‘hovering’ model hawkmoth. *Phil. Trans. R. Soc. Lond. B* **352**, 329–340. (doi:10.1098/rstb.1997.0024)
35. Willmott AP, Ellington CP, Thomas ALR. 1997 Flow visualization and unsteady aerodynamics in the flight of the hawkmoth, *Manduca sexta*. *Phil. Trans. R. Soc. Lond. B* **352**, 303–316. (doi:10.1098/rstb.1997.0022)
36. Shyy W, Aono H, Chimakurthi SK, Trizila P, Kang C, Cesnik CES, Liu H. 2010 Recent progress in flapping wing aerodynamics and aeroelasticity. *Prog. Aerosp. Sci.* **46**, 284–327. (doi:10.1016/j.paerosci.2010.01.001)
37. Anderson JD. 1991 *Fundamentals of aerodynamics*. New York, NY: McGraw Hill.
38. McCroskey WJ, McAlister KW, Carr LW, Pucci SL. 1982 An experimental study of dynamic stall on advanced airfoil section. NASA Technical Memorandum 84245.
39. Sane SP. 2003 The aerodynamics of insect flight. *J. Exp. Biol.* **206**, 4191–4208. (doi:10.1242/jeb.00663)
40. Scoble MJ. 1992 *The Lepidoptera*. New York, NY: Oxford University Press.
41. Vogel S. 2013 *Comparative biomechanics*. New Jersey, NY: Princeton University Press.
42. Dudley R. 2002 *The biomechanics of insect flight: form, function, evolution*. Princeton, NJ: Princeton University Press.
43. Lian Y, Broering T, Hord K, Prater R. 2014 The characterization of tandem and corrugated wings. *Prog. Aerosp. Sci.* **65**, 41–69. (doi:10.1016/j.paerosci.2013.08.001)
44. Usherwood JR, Lehmann F-O. 2008 Phasing of dragonfly wings can improve aerodynamic efficiency by removing swirl. *J. R. Soc. Interface* **5**, 1303–1307. (doi:10.1098/rsif.2008.0124)
45. Wang ZJ, Russell RD. 2007 Effect of forewind and hindwing interactions on aerodynamic forces and power in hovering dragonfly flight. *Phys. Rev. Lett.* **99**, 148101. (doi:10.1103/PhysRevLett.99.148101)
46. Maybury WJ, Lehmann F-O. 2004 The fluid dynamics of flight control by kinematic phase lag variation between two robotic insect wings. *J. Exp. Biol.* **207**, 4707–4726. (doi:10.1242/jeb.01319)
47. Zhang J, Lu X-Y. 2009 Aerodynamic performance due to forewing and hindwing interaction in gliding dragonfly flight. *Phys. Rev. E* **80**, 017302. (doi:10.1103/PhysRevE.80.017302)
48. Sun M, Lan SL. 2004 A computational study of the aerodynamic forces and power requirements of dragonfly (*Aeschna juncea*) hovering. *J. Exp. Biol.* **207**, 1887–1901. (doi:10.1242/jeb.00969)
49. Wang JK, Sun M. 2005 A computational study of the aerodynamics and forewing–hindwing interaction of a model dragonfly in forward flight. *J. Exp. Biol.* **208**, 3785–3804. (doi:10.1242/jeb.01852)
50. Rüppell G. 1989 Kinematic analysis of symmetrical flight manoeuvres of Odonata. *J. Exp. Biol.* **144**, 13–42.
51. Alexander DEE. 1984 Unusual phase relationships between the forewings and hindwings in flying dragonflies. *J. Exp. Biol.* **109**, 379–383.
52. Thomas ALR, Taylor GK, Srygley RB, Nudds RL, Bomphrey RJ. 2004 Dragonfly flight: free-flight and tethered flow visualizations reveal a diverse array of unsteady lift-generating mechanisms, controlled primarily via angle of attack. *J. Exp. Biol.* **207**, 4299–4323. (doi:10.1242/jeb.01262)
53. Koehler C, Liang Z, Gaston Z, Wan H, Dong H. 2012 3D reconstruction and analysis of wing deformation in free-flying dragonflies. *J. Exp. Biol.* **215**, 3018–3027. (doi:10.1242/jeb.069005)
54. Wakeling JM, Ellington CP. 1997 Dragonfly flight III. Lift and power requirements. *J. Exp. Biol.* **200**, 543–600.

55. Fu J, Hefler C, Qiu H, Shyy W. 2014 Effects of aspect ratio on flapping wing aerodynamics in animal flight. *Acta Mech. Sin.* **30**, 776–786. (doi:10.1007/s10409-014-0120-z)
56. Rees CJC. 1975 Form and function in corrugated insect wings. *Nature* **256**, 200–203. (doi:10.1038/256200a0)
57. Combes SA. 2010 Materials, structure, and dynamics of insect wings as bioinspiration for MAVs. In *Encyclopedia of aerospace engineering* (eds R Blockley, W Shyy), pp. 1–10. Chichester, UK: John Wiley and Sons, Ltd.
58. Jongerius SR, Lentink D. 2010 Structural analysis of a dragonfly wing. *Exp. Mech.* **50**, 1323–1334. (doi:10.1007/s11340-010-9411-x)
59. Kesel AB. 2000 Aerodynamic characteristics of dragonfly wing sections compared with technical aerofoils. *J. Exp. Biol.* **203**, 3125–3135.
60. Luo G, Sun M. 2005 Effects of corrugation and wing planform on the aerodynamic force production of sweeping model insect wings. *Acta Mech. Sin.* **21**, 531–541. (doi:10.1007/s10409-005-0072-4)
61. Meng XG, Xu L, Sun M. 2011 Aerodynamic effects of corrugation in flapping insect wings in hovering flight. *J. Exp. Biol.* **214**, 432–444. (doi:10.1242/jeb.046375)
62. Buckholz RH. 1986 The functional role of wing corrugations in living systems. *J. Fluids Eng.* **108**, 93. (doi:10.1115/1.3242550)
63. Murphy J, Hu H. 2009 An experimental investigation on a bio-inspired corrugated airfoil. In *AIAA-2009-1087, 47th AIAA Aerospace Sciences Meeting, Orlando, FL, 5–8 January*. Reston, VA: AIAA.
64. Vargas A, Mittal R, Dong H. 2008 A computational study of the aerodynamic performance of a dragonfly wing section in gliding flight. *Bioinspir. Biomim.* **3**, 026004. (doi:10.1088/1748-3182/3/2/026004)
65. Weis-Fogh T, Weis-fogh BYT, Weis-Fogh T. 1972 Energetics of hovering flight in hummingbirds and in drosophila. *J. Exp. Biol.* **56**, 79–104.
66. Shyy W, Berg M, Ljungqvist D. 1999 Flapping and flexible wings for biological and micro air vehicles. *Prog. Aerosp. Sci.* **35**, 455–505. (doi:10.1016/S0376-0421(98)00016-5)
67. Theodorsen T. 1935 General theory of aerodynamic instability and the mechanism of flutter. *NACA Rep.* **496**, 1–26.
68. von Karman T, Sears WR. 1938 Airfoil theory for non-uniform motion. *J. Aeronaut. Sci.* **5**, 379–390. (doi:10.2514/8.674)
69. Küssner HG. 1936 Zusammenfassender bericht ueber den instationaeren auftrieb von fluegeln. *Luftfahrtforschung* **13**, 410.
70. Usherwood JR, Ellington CP. 2002 The aerodynamics of revolving wings I. Model hawkmoth wings. *J. Exp. Biol.* **205**, 1547–1564.
71. Berman GJ, Wang ZJ. 2007 Energy-minimizing kinematics in hovering insect flight. *J. Fluid Mech.* **582**, 153. (doi:10.1017/S0022112007006209)
72. Whitney JP, Wood RJ. 2010 Aeromechanics of passive rotation in flapping flight. *J. Fluid Mech.* **660**, 197–220. (doi:10.1017/S002211201000265X)
73. Kang C, Shyy W. 2014 Analytical model for instantaneous lift and shape deformation of an insect-scale flapping wing in hover. *J. R. Soc. Interface* **11**, 20140933. (doi:10.1098/rsif.2014.0933)
74. Kang C, Shyy W. 2013 Scaling law and enhancement of lift generation of an insect-size hovering flexible wing. *J. R. Soc. Interface* **10**, 20130361. (doi:10.1098/rsif.2013.0361)
75. Shih CC, Buchanan HJ. 1971 The drag on oscillating flat plates in liquids at low Reynolds numbers. *J. Fluid Mech.* **48**, 229–239. (doi:10.1017/S0022112071001563)
76. Beatus T, Cohen I. 2015 Wing-pitch modulation in maneuvering fruit flies is explained by an interplay between aerodynamics and a torsional spring. *Phys. Rev. E* **92**, 022712. (doi:10.1103/PhysRevE.92.022712)
77. Taha HE, Hajj MR, Beran PS. 2014 State-space representation of the unsteady aerodynamics of flapping flight. *Aerosp. Sci. Technol.* **34**, 1–11. (doi:10.1016/j.ast.2014.01.011)
78. Nakata T, Liu H, Bompfrey RJ. 2015 A CFD-informed quasi-steady model of flapping wing aerodynamics. *J. Fluid Mech.* **783**, 323–343. (doi:10.1017/jfm.2015.537)
79. Curet OM, Swartz SM, Breuer KS. 2013 An aeroelastic instability provides a possible basis for the transition from gliding to flapping flight. *J. R. Soc. Interface* **10**, 20120940. (doi:10.1098/rsif.2012.0940)
80. Combes SA, Daniel TL. 2003 Flexural stiffness in insect wings I. Scaling and the influence of wing venation. *J. Exp. Biol.* **206**, 2979–2987. (doi:10.1242/jeb.00523)

81. Combes SA, Daniel TL. 2003 Flexural stiffness in insect wings II. Spatial distribution and dynamic wing bending. *J. Exp. Biol.* **206**, 2989–2997. (doi:10.1242/jeb.00524)
82. Azuma A. 2006 *The biokinetics of flying and swimming*, 2nd edn. Reston, VA: AIAA Inc.
83. Tu M, Dickinson M. 1994 Modulation of negative work output from a steering muscle of the blowfly *Calliphora vicina*. *J. Exp. Biol.* **192**, 207–224.
84. Lehmann FO, Götz KG. 1996 Activation phase ensures kinematic efficacy in flight-steering muscles of *Drosophila melanogaster*. *J. Comp. Physiol. A* **179**, 311–322. (doi:10.1007/BF00194985)
85. Fry SN, Sayaman R, Dickinson MH. 2005 The aerodynamics of hovering flight in *Drosophila*. *J. Exp. Biol.* **208**, 2303–2318. (doi:10.1242/jeb.01612)
86. Sane SP, Dickinson MH. 2001 The control of flight force by a flapping wing: lift and drag production. *J. Exp. Biol.* **204**, 2607–2626.
87. Lehmann F-O, Gorb S, Nasir N, Schützner P, Schützner P. 2011 Elastic deformation and energy loss of flapping fly wings. *J. Exp. Biol.* **214**, 2949–2961. (doi:10.1242/jeb.045351)
88. Pornsin-Sirirak TN, Tai YC, Nassef H, Ho CM. 2001 Titanium-alloy MEMS wing technology for a micro aerial vehicle application. *Sensors Actuators A Phys.* **89**, 95–103. (doi:10.1016/S0924-4247(00)00527-6)
89. Tennekes H. 2009 *The simple science of flight: from insects to jumbo jets*. Cambridge, MA: MIT Press.
90. Jane FT. 1997 *Jane's all the World's aircraft*. London, UK: Sampson Low, Marston and Company.
91. Liu T. 2006 Comparative scaling of flapping- and fixed-wing flyers. *AIAA J.* **44**, 24–33. (doi:10.2514/1.4035)
92. Ristroph L, Ristroph G, Morozova S, Bergou AJ, Chang S, Guckenheimer J, Wang ZJ, Cohen I. 2013 Active and passive stabilization of body pitch in insect flight. *J. R. Soc. Interface* **10**, 20130237. (doi:10.1098/rsif.2013.0237)
93. Pennycuik CJ. 1975 Mechanics of flight. *Avian Biol.* **5**, 1–75. (doi:10.1016/B978-0-12-249405-5.50009-4)
94. Daniel TL, Combes SA. 2002 Flexible wings and fins: bending by inertial or fluid-dynamic forces? *Integr. Comp. Biol.* **42**, 1044–1049. (doi:10.1093/icb/42.5.1044)
95. Pornsin-Sirirak TN, Tai Y-C, Ho C-M, Keennon M. 2001 Microbat: A palm-sized electrically powered ornithopter. In *Proc. of NASA/JPL Workshop on Biomimetic Robotics, Pasadena, CA, 14–17 August*, pp. 14–17.
96. Tanaka H, Wood RJ. 2010 Fabrication of corrugated artificial insect wings using laser micromachined molds. *J. Micromech. Microeng.* **20**, 75008. (doi:10.1088/0960-1317/20/7/075008)
97. Meng K *et al.* 2012 The design and micromachining of an electromagnetic MEMS flapping-wing micro air vehicle. *Microsyst. Technol.* **18**, 127–136. (doi:10.1007/s00542-011-1388-6)
98. Shang JK, Combes SA, Finio BM, Wood RJ. 2009 Artificial insect wings of diverse morphology for flapping-wing micro air vehicles. *Bioinspir. Biomim.* **4**, 36002. (doi:10.1088/1748-3182/4/3/036002)
99. Tanaka H, Okada H, Shimasue Y, Liu H. 2015 Flexible flapping wings with self-organized microwrinkles. *Bioinspir. Biomim.* **10**, 46005. (doi:10.1088/1748-3190/10/4/046005)
100. Tanaka H, Whitney JP, Wood RJ. 2011 Effect of flexural and torsional wing flexibility on lift generation in hoverfly flight. *Integr. Comp. Biol.* **51**, 142–150. (doi:10.1093/icb/icr051)
101. Perez-Rosado A, Gehlhar RD, Nolen S, Gupta SK, Bruck HA. 2015 Design, fabrication, and characterization of multifunctional wings to harvest solar energy in flapping wing air vehicles. *Smart Mater. Struct.* **24**, 65042. (doi:10.1088/0964-1726/24/6/065042)
102. Agrawal A, Agrawal SK. 2009 Design of bio-inspired flexible wings for flapping-wing micro-sized air vehicle applications. *Adv. Robot.* **23**, 979–1002. (doi:10.1163/156855309X443133)
103. Lentink D, Jongerius SR, Bradshaw NL. 2010 The scalable design of flapping micro-air vehicles inspired by insect flight. In *Flying insects and robots* (eds D Floreano, J-C Zufferey, MV Srinivasan, C Ellington), pp. 185–205. Berlin, Germany: Springer.
104. Wood RJ. 2007 Design, fabrication, and analysis of a 3DOF, 3 cm flapping-wing MAV. In *Intelligent Robots and Systems, 2007. IROS 2007. IEEE/RSJ Int. Conf., San Diego, CA, 29 October–2 November*, pp. 1576–1581. Piscataway, NJ: IEEE.
105. Ma KY, Chirarattananon P, Fuller SB, Wood RJ 2013 Controlled flight of a biologically inspired, insect-scale robot. *Science* **340**, 603–607. (doi:10.1126/science.1231806)

106. Ho S, Nassef H, Pornsinsirak N, Tai Y-C, Ho C-M. 2003 Unsteady aerodynamics and flow control for flapping wing flyers. *Prog. Aerosp. Sci.* **39**, 635–681. (doi:10.1016/j.paerosci.2003.04.001)
107. Sunada S, Yasuda T, Yasuda K, Kawachi K. 2002 Comparison of wing characteristics at an ultralow Reynolds number. *J. Aircr.* **39**, 331–338. (doi:10.2514/2.2931)
108. Watman D, Furukawa T. 2009 A parametric study of flapping wing performance using a robotic flapping wing. In *Robotics and Automation, 2009. ICRA'09. IEEE Int. Conf., 12–17 May, Kobe, Japan*, pp. 3638–3643. Piscataway, NJ: IEEE.
109. Gremillion G, Humbert JS, Krapp HG. 2014 Bio-inspired modeling and implementation of the ocelli visual system of flying insects. *Biol. Cybern.* **108**, 735–746. (doi:10.1007/s00422-014-0610-x)
110. Nguyen Q-V, Chan WL, Debiasi M. 2015 An insect-inspired flapping wing micro air vehicle with double wing clap-fling effects and capability of sustained hovering. In *SPIE Smart Structures and Materials + Nondestructive Evaluation and Health Monitoring, San Diego, CA, 8 March*, pp. 94290U. Bellingham, WA: SPIE.
111. Kim D-K, Kim H-I, Han J-H, Kwon K-J. 2007 Experimental investigation on the aerodynamic characteristics of a bio-mimetic flapping wing with macro-fiber composites. *J. Intell. Mater. Syst. Struct.* **19**, 423–431. (doi:10.1177/1045389X07083618)
112. Hu H, Kumar AG, Abate G, Albertani R. 2009 An experimental study of flexible membrane wings in flapping flight. In *47th AIAA Aerospace Sciences Meeting Including the New Horizons Forum and Aerospace Exposition, Orlando, FL, 5–8 January 2009*, pp. 2009–2876. Reston, VA: AIAA.
113. Groen M, Bruggeman B, Remes B, Ruijsink R, Van Oudheusden BW, Bijl H. 2010 Improving flight performance of the flapping wing MAV Delfly II. In *Int. Micro Air Vehicle Conf. and Competition (IMAV 2010), Braunschweig, Germany, 6–9 July*.
114. Wood RJ, Avadhanula S, Sahai R, Steltz E, Fearing RS. 2008 Microrobot design using fiber reinforced composites. *J. Mech. Des.* **130**, 52304. (doi:10.1115/1.2885509)
115. Sreetharan PS, Whitney JP, Strauss MD, Wood RJ. 2012 Monolithic fabrication of millimeter-scale machines. *J. Micromech. Microeng.* **22**, 55027. (doi:10.1088/0960-1317/22/5/055027)
116. Sahai R, Galloway KC, Karpelson M, Wood RJ. 2012 A flapping-wing micro air vehicle with interchangeable parts for system integration studies. In *Intelligent Robots and Systems (IROS), 2012 IEEE/RSJ Int. Conf. on Vilamoura, Portugal, 7–12 October*, pp. 501–506. Piscataway, NJ: IEEE.
117. Sahai R, Galloway KC, Wood RJ. 2013 Elastic element integration for improved flapping-wing micro air vehicle performance. *Robot. IEEE Trans.* **29**, 32–41. (doi:10.1109/TRO.2012.2218936)
118. Bontemps A, Vanneste T, Paquet JB, Dietsch T, Grondel S, Cattan E. 2013 Design and performance of an insect-inspired nano air vehicle. *Smart Mater. Struct.* **22**, 14008. (doi:10.1088/0964-1726/22/1/014008)
119. Campolo D, Azhar M, Lau G-K, Sitti M. 2014 Can DC motors directly drive flapping wings at high frequency and large wing strokes? *Mech. IEEE/ASME Trans.* **19**, 109–120. (doi:10.1109/TMECH.2012.2222432)
120. Azhar M, Campolo D, Lau G-K, Hines L, Sitti M. 2013 Flapping wings via direct-driving by DC motors. In *Robotics and Automation (ICRA), 2013 IEEE Int. Conf. Karlsruhe, Germany, 6–10 May*, pp. 1397–1402. Piscataway, NJ: IEEE.
121. Roll J, Cheng B, Deng X (eds). 2013 Design, fabrication, and experiments of an electromagnetic actuator for flapping wing micro air vehicles. In *Robotics and Automation (ICRA), 2013 IEEE Int. Conf., Karlsruhe, Germany, 6–10 May*, pp. 809–815.
122. Keennon M, Klingebiel K, Won H, Andriukov A. 2012 Development of the nano hummingbird: a tailless flapping wing micro air vehicle. In *AIAA-2012-0588, 50th AIAA Aerospace Sciences Meeting, Nashville, TN, 9–12 January*. Reston, VA: AIAA.
123. Eldredge JD, Pisani D. 2008 Passive locomotion of a simple articulated fish-like system in the wake of an obstacle. *J. Fluid Mech.* **607**, 279–288. (doi:10.1017/S0022112008002218)
124. Ramanarivo S, Godoy-Diana R, Thiria B. 2011 Rather than resonance, flapping wing flyers may play on aerodynamics to improve performance. *Proc. Natl Acad. Sci. USA* **108**, 5964–5969. (doi:10.1073/pnas.1017910108)
125. Yin B, Luo H. 2010 Effect of wing inertia on hovering performance of flexible flapping wings. *Phys. Fluids* **22**, 111902. (doi:10.1063/1.3499739)

126. Vanella M, Fitzgerald T, Preidikman S, Balaras E, Balachandran B. 2009 Influence of flexibility on the aerodynamic performance of a hovering wing. *J. Exp. Biol.* **212**, 95–105. (doi:10.1242/jeb.016428)
127. Dewey PA, Boschitsch BM, Moored KW, Stone HA, Smits AJ. 2013 Scaling laws for the thrust production of flexible pitching panels. *J. Fluid Mech.* **732**, 29–46. (doi:10.1017/jfm.2013.384)
128. Lamb H. 1945 *Hydrodynamics*, 6th edn. New York, NY: Dover.
129. Saffman PG. 1995 *Vortex dynamics*. New York, NY: Cambridge University Press.
130. Thiria B, Godoy-Diana R. 2010 How wing compliance drives the efficiency of self-propelled flapping flyers. *Phys. Rev. E* **82**, 15303. (doi:10.1103/PhysRevE.82.015303)
131. Lua KB, Lim TT, Yeo KS. 2011 Effect of wing-wake interaction on aerodynamic force generation on a 2D flapping wing. *Exp. Fluids* **51**, 177–195. (doi:10.1007/s00348-010-1032-8)
132. Sridhar M, Kang C. 2015 Aerodynamic performance of two-dimensional, chordwise flexible flapping wings at fruit fly scale in hover flight. *Bioinspir. Biomim.* **10**, 036007. (doi:10.1088/1748-3190/10/3/036007)
133. Altshuler DL, Dickson WB, Vance JT, Roberts SP, Dickinson MH. 2005 Short-amplitude high-frequency wing strokes determine the aerodynamics of honeybee flight. *Proc. Natl Acad. Sci. USA* **102**, 18 213–18 218. (doi:10.1073/pnas.0506590102)
134. Chen J-S, Chen J-Y, Chou Y-F. 2008 On the natural frequencies and mode shapes of dragonfly wings. *J. Sound Vib.* **313**, 643–654. (doi:10.1016/j.jsv.2007.11.056)
135. Sunada S, Zeng L, Kawachi K. 1998 The relationship between dragonfly wing structure and torsional deformation. *J. Theor. Biol.* **193**, 39–45. (doi:10.1006/jtbi.1998.0678)
136. Alben S, Shelley M, Zhang J. 2002 Drag reduction through self-similar bending of a flexible body. *Nature* **420**, 479–481. (doi:10.1038/nature01232)
137. Sun M. 2014 Insect flight dynamics: stability and control. *Rev. Mod. Phys.* **86**, 615–646. (doi:10.1103/RevModPhys.86.615)
138. Morison JR, O'Brien MP, Johnson JW, Schaaf SA. 1950 The force exerted by surface waves on piles. *Pet. Trans.* **189**, 149–154.
139. Nakata T, Liu H. 2012 Aerodynamic performance of a hovering hawkmoth with flexible wings: a computational approach. *Proc. R. Soc. B* **279**, 722–731. (doi:10.1098/rspb.2011.1023)
140. Mountcastle AM, Combes SA. 2013 Wing flexibility enhances load-lifting capacity in bumblebees. *Proc. R. Soc. B* **280**, 20130531. (doi:10.1098/rspb.2013.0531)
141. Wootton RJ. 1993 Leading edge section and asymmetric twisting in the wings of flying butterflies. *J. Exp. Biol.* **180**, 105–117.
142. Walshe DEJ. 1972 *Wind-excited oscillations of structures*. London, UK: Her Majesty's Stationery Office.
143. Karpelson M, Wei G-Y, Wood RJ. 2008 A review of actuation and power electronics options for flapping-wing robotic insects. In *2008 IEEE International Conf. on Robotics and Automation, Pasadena, CA, 19–23 May*, pp. 779–786. Piscataway, NJ: IEEE.
144. Floreano D, Zufferey J-C, Srinivasan MV, Ellington C. 2009 *Flying insects and robots*. Berlin, Germany: Springer.
145. Ruffier F, Franceschini N. 2005 Optic flow regulation: the key to aircraft automatic guidance. *Robot. Automous Syst.* **50**, 177–194. (doi:10.1016/j.robot.2004.09.016)
146. Shyy W, Jenkins DA, Smith RW. 1997 Study of adaptive shape airfoils at low Reynolds number in oscillatory flow. *AIAA J.* **35**, 1545–1548. (doi:10.2514/2.7484)
147. Shyy W, Klevebring F, Nilsson M, Sloan J, Carroll B, Fuentes C. 1999 A study of rigid and flexible low Reynolds number airfoils. *J. Aircr.* **36**, 523–529. (doi:10.2514/2.2487)
148. Lian Y, Shyy W. 2007 Aerodynamics of low Reynolds number plunging airfoil under gusty environment. In *45th AIAA Aerospace Sciences Meeting and Exhibit, Reno, NV, 8–11 January, AIAA-2007-71*. Reston, VA: AIAA.
149. Lian Y. 2009 Numerical study of a flapping airfoil in gusty environments. In *27th AIAA Appl. Aerodyn. Conf., San Antonio, TX, 22–25 June*. Reston, VA: AIAA.
150. Jones M, Yamaleev NK. 2012 The effect of a gust on the flapping wing performance. In *50th AIAA Aerospace Sciences Meeting including the New Horizons Forum and Aerospace Exposition, Nashville, TN, 9–12 January*. Reston, VA: AIAA.
151. Jones MA. 2013 *CFD analysis and design optimization of flapping wing flows*. PhD Dissertation North Carolina A&T State University, Greensboro, NC.
152. Fisher A. 2013 *The effect of freestream turbulence on fixed and flapping micro air vehicle wings*. PhD Thesis, Aerospace, Mechanical and Manufacturing Engineering, RMIT University, Melbourne, Australia.

153. Ortega-Jimenez VM, Greeter JSM, Mittal R, Hedrick TL. 2013 Hawkmoth flight stability in turbulent vortex streets. *J. Exp. Biol.* **216**, 4567–4579. (doi:10.1242/jeb.089672)
154. Ravi S, Crall JD, Fisher A, Combes SA. 2013 Rolling with the flow: bumblebees flying in unsteady wakes. *J. Exp. Biol.* **216**, 4299–4309. (doi:10.1242/jeb.090845)
155. Ravi S, Crall JD, McNeilly L, Gagliardi SF, Biewener AA, Combes SA. 2015 Hummingbird flight stability and control in freestream turbulent winds. *J. Exp. Biol.* **218**, 1444–1452. (doi:10.1242/jeb.114553)
156. Combes SA, Dudley R. 2009 Turbulence-driven instabilities limit insect flight performance. *Proc. Natl Acad. Sci. USA* **106**, 9105–9108. (doi:10.1073/pnas.0902186106)
157. Kim EJ, Wolf M, Ortega-Jimenez VM, Cheng SH, Dudley R. 2014 Hovering performance of Anna's hummingbirds (*Calypte anna*) in ground effect. *J. R. Soc. Interface* **11**, 20140505. (doi:10.1098/rsif.2014.0505)
158. Ortega-Jimenez VM, Sapir N, Wolf M, Variano EA, Dudley R. 2014 Into turbulent air: size-dependent effects of von Karman vortex streets on hummingbird flight kinematics and energetics. *Proc. R. Soc. B* **281**, 20140180. (doi:10.1098/rspb.2014.0180)
159. Watkins S, Ravi S, Loxton B. 2010 The effect of turbulence on the aerodynamics of low Reynolds number wings. *Eng. Lett.* **18**, 279–285.
160. Vance JT, Faruque I, Humbert JS. 2013 Kinematic strategies for mitigating gust perturbations in insects. *Bioinspir. Biomim.* **8**, 016004. (doi:10.1088/1748-3182/8/1/016004)
161. Ortega-Jimenez VM, Mittal R, Hedrick TL. 2014 Hawkmoth flight performance in tornado-like whirlwind vortices. *Bioinspir. Biomim.* **9**, 025003. (doi:10.1088/1748-3182/9/2/025003)
162. Ravi S, Crall JD, Gagliardi S, McNeilly L, Biewener AA, Combes SA. 2014 Hummingbird flight stability and control in freestream turbulent winds. *J. Exp. Biol.* **218**, 1444–1452. (doi:10.1242/jeb.114553)
163. Hedrick TL. 2011 Damping in flapping flight and its implications for manoeuvring, scaling and evolution. *J. Exp. Biol.* **214**, 4073–4081. (doi:10.1242/jeb.047001)
164. Hedrick TL, Cheng B, Deng X. 2009 Wingbeat time and the scaling of passive rotational damping in flapping flight. *Science* **324**, 252–255. (doi:10.1126/science.1168431)
165. Alexander DE, Vogel S. 2004 *Nature's flyers: birds, insects, and the biomechanics of flight*. 1st edn. Baltimore, MD: JHU Press.
166. Taha HE, Nayfeh AH, Hajj MR. 2014 Effect of the aerodynamic-induced parametric excitation on the longitudinal stability of hovering MAVs/insects. *Nonlinear Dyn.* **78**, 2399–2408. (doi:10.1007/s11071-014-1596-6)
167. Cheng B, Fry SN, Huang Q, Dickson WB, Dickinson MH, Deng X. 2009 Turning dynamics and passive damping in flapping flight. In *2009 IEEE Int. Conf. on Robotics and Automation, Kobe, Japan, 12–17 May*, pp. 1889–1896. Piscataway, NJ: IEEE.
168. Humbert JS, Faruque IA. 2011 Analysis of insect-inspired wingstroke kinematic perturbations for longitudinal control. *J. Guid. Control. Dyn.* **34**, 618–623. (doi:10.2514/1.51912)
169. Taha HE, Nayfeh AH, Hajj MR. 2013 Saturation-based actuation for flapping MAVs in hovering and forward flight. *Nonlinear Dyn.* **73**, 1125–1138. (doi:10.1007/s11071-013-0857-0)
170. Ellington CP. 1984 The aerodynamics of hovering insect flight. VI. Lift and power requirements. *Phil. Trans. R. Soc. Lond. B* **305**, 145–181. (doi:10.1098/rstb.1984.0054)
171. Dillon ME, Dudley R. 2014 Surpassing Mt. Everest: extreme flight performance of alpine bumble-bees. *Biol. Lett.* **10**, 20130922. (doi:10.1098/rsbl.2013.0922)
172. Altshuler DL, Dudley R. 2003 Kinematics of hovering hummingbird flight along simulated and natural elevational gradients. *J. Exp. Biol.* **206**, 3139–3147. (doi:10.1242/jeb.00540)
173. Sefati S, Neveln ID, Roth E, Mitchell TRT, Snyder JB, Maciver MA, Fortune ES, Cowan NJ. 2013 Mutually opposing forces during locomotion can eliminate the tradeoff between maneuverability and stability. *Proc. Natl Acad. Sci. USA* **110**, 18798–18803. (doi:10.1073/pnas.1309300110)
174. Orłowski CT, Girard AR. 2012 Dynamics, stability, and control analyses of flapping wing micro-air vehicles. *Prog. Aerosp. Sci.* **51**, 18–30. (doi:10.1016/j.paerosci.2012.01.001)
175. Liang B, Sun M. 2013 Nonlinear flight dynamics and stability of hovering model insects. *J. R. Soc. Interface* **10**, 20130269. (doi:10.1098/rsif.2013.0269)
176. Kumar V, Michael N. 2012 Opportunities and challenges with autonomous micro aerial vehicles. *Int. J. Rob. Res.* **31**, 1279–1291. (doi:10.1177/0278364912455954)

177. Martin P, Salaun E. 2010 The true role of accelerometer feedback in quadrotor control. In *Robotics and Automation (ICRA), 2010 IEEE Int. Conf., Anchorage, AK, 3–7 May*, pp. 1623–1629. Piscataway, NJ: IEEE.
178. Pringle JWS. 1948 The gyroscopic mechanism of the halteres of Diptera. *Phil. Trans. R. Soc. Lond. B* **233**, 347–384. (doi:10.1098/rstb.1948.0007)
179. Dickinson MH. 1999 Haltere-mediated equilibrium reflexes of the fruit fly, *Drosophila melanogaster*. *Phil. Trans. R. Soc. Lond. B* **354**, 903–916. (doi:10.1098/rstb.1999.0442)
180. Hengstenberg R. 1988 Mechanosensory control of compensatory head roll during flight in the blowfly *Calliphora erythrocephala* Meig. *J. Comp. Physiol. A* **163**, 151–165. (doi:10.1007/BF00612425)
181. Dickson WB, Straw AD, Poelma C, Dickinson MH. 2006 An integrative model of insect flight control. In *Proc. of the 44th AIAA Aerospace Sciences Meeting and Exhibit, Reno, NV, 9–12 January*, pp. 31–38. Reston, VA: AIAA.
182. Fuller SB, Karpelson M, Censi A, Ma KY, Wood RJ. 2014 Controlling free flight of a robotic fly using an onboard vision sensor inspired by insect ocelli. *J. R. Soc. Interface* **11**, 20140281. (doi:10.1098/rsif.2014.0281)
183. Fox JL, Fairhall AL, Daniel TL. 2010 Encoding properties of haltere neurons enable motion feature detection in a biological gyroscope. *Proc. Natl Acad. Sci. USA* **107**, 3840–3845. (doi:10.1073/pnas.0912548107)
184. Sane SP, Dieudonné A, Willis MA, Daniel TL. 2007 Antennal mechanosensors mediate flight control in moths. *Science* **315**, 863–866. (doi:10.1126/science.1133598)
185. Hinterwirth AJ, Daniel TL. 2010 Antennae in the hawkmoth *Manduca sexta* (Lepidoptera, Sphingidae) mediate abdominal flexion in response to mechanical stimuli. *J. Comp. Physiol. A* **196**, 947–956. (doi:10.1007/s00359-010-0578-5)
186. Kalmus H. 1945 Correlations between flight and vision, and particularly between wings and ocelli, in jksects. *Proc. R. Entomol. Soc. A* **20**, 84–96. (doi:10.1111/j.1365-3032.1945.tb01072.x)
187. Parsons MM, Krapp HG, Laughlin SB. 2010 Sensor fusion in identified visual interneurons. *Curr. Biol.* **20**, 624–628. (doi:10.1016/j.cub.2010.01.064)
188. Taylor CP. 1981 Contribution of compound eyes and ocelli to steering of locusts in flight: I. Behavioural analysis. *J. Exp. Biol.* **93**, 1–18.
189. Srinivasan MV, Moore RJD, Thurrowgood S, Soccol D, Bland D. 2012 *From biology to engineering: insect vision and applications to robotics*. Vienna, Austria: Springer.
190. Chahl J, Mizutani A. 2012 Biomimetic attitude and orientation sensors. *Sensors J. IEEE* **12**, 289–297. (doi:10.1109/JSEN.2010.2078806)
191. Chahl J, Thakoor S, Le Bouffant N, Stange G, Srinivasan MV, Hine B, Zornetzer S. 2003 Bioinspired engineering of exploration systems: a horizon sensor/attitude reference system based on the dragonfly ocelli for mars exploration applications. *J. Robot. Syst.* **20**, 35–42. (doi:10.1002/rob.10068)
192. Wendel J, Meister O, Schlaile C, Trommer GF. 2006 An integrated GPS/MEMS-IMU navigation system for an autonomous helicopter. *Aerosp. Sci. Technol.* **10**, 527–533. (doi:10.1016/j.ast.2006.04.002)
193. Fuller SB, Helbling EF, Chirarattananon P, Wood RJ. 2014 Using a MEMS gyroscope to stabilize the attitude of a fly-sized hovering robot. In *IMAV 2014: Int. Micro Air Vehicle Conf. and Competition 2014, Delft, The Netherlands, 12–15 August*. IMAV.
194. Nakata T, Liu H, Tanaka Y, Nishihashi N, Wang X, Sato A. 2011 Aerodynamics of a bio-inspired flexible flapping-wing micro air vehicle. *Bioinspir. Biomim.* **6**, 45002. (doi:10.1088/1748-3182/6/4/045002)
195. Schneider D. 1964 Insect antennae. *Annu. Rev. Entomol.* **9**, 103–122. (doi:10.1146/annurev.en.09.010164.000535)
196. Schütz S, Weissbecker B, Hummel HE, Apel K-H, Schmitz H, Bleckmann H. 1999 Insect antenna as a smoke detector. *Nature* **398**, 298–299. (doi:10.1038/18585)
197. Gewecke M. 1974 The antennae of insects as air-current sense organs and their relationship to the control of flight. In *Experimental analysis of insect behaviour*, pp. 100–113. Berlin, Germany: Springer.
198. Mamiya A, Straw AD, Tómasson E, Dickinson MH. 2011 Active and passive antennal movements during visually guided steering in flying *Drosophila*. *J. Neurosci.* **31**, 6900–6914. (doi:10.1523/JNEUROSCI.0498-11.2011)
199. Taylor GK, Krapp HG. 2007 Sensory systems and flight stability: what do insects measure and why? *Adv. In Insect Phys.* **34**, 231–316. (doi:10.1016/S0065-2806(07)34005-8)

200. Rohrseitz N, Fry SN. 2011 Behavioural system identification of visual flight speed control in *Drosophila melanogaster*. *J. R. Soc. Interface* **8**, 171–185. (doi:10.1098/rsif.2010.0225)
201. Fuller SB, Straw AD, Peek MY, Murray RM, Dickinson MH. 2014 Flying *Drosophila* stabilize their vision-based velocity controller by sensing wind with their antennae. *Proc. Natl Acad. Sci. USA* **111**, E1182–E1191. (doi:10.1073/pnas.1323529111)
202. Najafi K. 2012 Biomimetic hair sensors: utilizing the third dimension. In *Sensors, 2012 IEEE, Taipei, Taiwan, 28–31 October*, pp. 1–4.
203. Wang Y-H, Lee C-Y, Chiang C-M. 2007 A MEMS-based air flow sensor with a free-standing micro-cantilever structure. *Sensors* **7**, 2389–2401. (doi:10.3390/s7102389)
204. Fuller SB, Sands A, Haggerty A, Karpelson M, Wood RJ. 2013 Estimating attitude and wind velocity using biomimetic sensors on a microbotic bee. In *Robotics and Automation (ICRA), 2013 IEEE Int. Conf., Karlsruhe, Germany, 6–10 May*, pp. 1374–1380. Piscataway, NJ: IEEE.
205. van Breugel F, Morgansen K, Dickinson MH. 2014 Monocular distance estimation from optic flow during active landing maneuvers. *Bioinspir. Biomim.* **9**, 25002. (doi:10.1088/1748-3182/9/2/025002)
206. Windsor SP, Bompfrey RJ, Taylor GK. 2014 Vision-based flight control in the hawkmoth *Hyles lineata*. *J. R. Soc. Interface* **11**, 20130921. (doi:10.1098/rsif.2013.0921)
207. Song YM *et al.* 2013 Digital cameras with designs inspired by the arthropod eye. *Nature* **497**, 95–99. (doi:10.1038/nature12083)
208. Baird E, Boeddeker N, Ibbotson MR, Srinivasan MV. 2013 A universal strategy for visually guided landing. *Proc. Natl Acad. Sci. USA* **110**, 18 686–18 691. (doi:10.1073/pnas.1314311110)
209. Muijres FT, Elzinga MJ, Melis JM, Dickinson MH. 2014 Flies evade looming targets by executing rapid visually directed banked turns. *Science* **344**, 172–177. (doi:10.1126/science.1248955)
210. Koenderink JJ, van Doorn AJ. 1987 Facts on optic flow. *Biol. Cybern.* **56**, 247–254. (doi:10.1007/BF00365219)
211. Karmeier K, Krapp HG, Egelhaaf M. 2003 Robustness of the tuning of fly visual interneurons to rotatory optic flow. *J. Neurophysiol.* **90**, 1626–1634. (doi:10.1152/jn.00234.2003)
212. Dyrh JP, Higgins CM. 2010 The spatial frequency tuning of optic-flow-dependent behaviors in the bumblebee *Bombus impatiens*. *J. Exp. Biol.* **213**, 1643–1650. (doi:10.1242/jeb.041426)
213. Baird E, Dacke M. 2012 Visual flight control in naturalistic and artificial environments. *J. Comp. Physiol. A* **198**, 869–876. (doi:10.1007/s00359-012-0757-7)
214. Srinivasan MV, Lehrer M, Kirchner WH, Zhang SW. 1991 Range perception through apparent image speed in freely flying honeybees. *Vis. Neurosci.* **6**, 519–535. (doi:10.1017/S09525238000136X)
215. Fry SN, Rohrseitz N, Straw AD, Dickinson MH. 2009 Visual control of flight speed in *Drosophila melanogaster*. *J. Exp. Biol.* **212**, 1120–1130. (doi:10.1242/jeb.020768)
216. Zingg S, Scaramuzza D, Weiss S, Siegwart R. 2010 MAV navigation through indoor corridors using optical flow. In *Robotics and Automation (ICRA), 2010 IEEE Int. Conf., Anchorage, AK, 3–7 May*, pp. 3361–3368. Piscataway, NJ: IEEE.
217. De Croon G, De Clercq KME, Ruijsink R, Remes B, De Wagter C. 2009 Design, aerodynamics, and vision-based control of the DelFly. *Int. J. Micro Air Veh.* **1**, 71–97. (doi:10.1260/175682909789498288)
218. LeCun Y, Bengio Y, Hinton G. 2015 Deep learning. *Nature* **521**, 436–444. (doi:10.1038/nature14539)
219. Achtelik M, Bachrach A, He R, Prentice S, Roy N. 2009 Stereo vision and laser odometry for autonomous helicopters in GPS-denied indoor environments. In *SPIE Defense, security, and sensing* (eds GR Gerhart, DW Gage, CM Shoemaker), pp. 733219. Unmanned Systems Technology XI. Orlando, FL, USA: SPIE.
220. Schmid K, Lutz P, Tomić T, Mair E, Hirschmüller H. 2014 Autonomous vision-based micro air vehicle for indoor and outdoor navigation. *J. F. Robot.* **31**, 537–570. (doi:10.1002/rob.21506)
221. Gerdes J *et al.* 2014 Robo Raven: a flapping-wing air vehicle with highly compliant and independently controlled wings. *Soft Robot.* **1**, 275–288. (doi:10.1089/soro.2014.0019)
222. Beyeler A, Zufferey J-C, Floreano D. 2009 Vision-based control of near-obstacle flight. *Auton. Robots* **27**, 201–219. (doi:10.1007/s10514-009-9139-6)

223. Duhamel P-EJ, Perez-Arancibia NO, Barrows GL, Wood RJ. 2013 Biologically inspired optical-flow sensing for altitude control of flapping-wing microrobots. *Mech. IEEE/ASME Trans.* **18**, 556–568. (doi:10.1109/TMECH.2012.2225635)
224. Expert F, Ruffier F. 2015 Flying over uneven moving terrain based on optic-flow cues without any need for reference frames or accelerometers. *Bioinspir. Biomim.* **10**, 26003. (doi:10.1088/1748-3182/10/2/026003)
225. Floreano D *et al.* 2013 Miniature curved artificial compound eyes. *Proc. Natl Acad. Sci. USA* **110**, 9267–9272. (doi:10.1073/pnas.1219068110)
226. Pericet-Camara R, Dobrzynski MK, Juston R, Viollet S, Leitel R, Mallot HA, Floreano D. 2015 An artificial elementary eye with optic flow detection and compositional properties. *J. R. Soc. Interface* **12**, 20150414. (doi:10.1098/rsif.2015.0414)
227. Ennos AR. 1989 The kinematics and aerodynamics of the free flight of some Diptera. *J. Exp. Biol.* **142**, 49–85.
228. Sadaf S, Reddy OV, Sane S, Hasan G. 2015 Neural Control Of Wing Coordination In Flies. *Curr. Biol.* **25**, 80–86. (doi:10.1016/j.cub.2014.10.069)
229. Srinivasan MV. 1977 A visually-evoked roll response in the housefly. *J. Comp. Physiol. A* **119**, 1–14. (doi:10.1007/BF00655868)
230. Preiss R, Spork P. 1994 Singificance of reafferent information on yaw rotation in the visual control of translator flight maneuvers in locusts. *Naturwissenschaften* **81**, 38–40. (doi:10.1007/BF01138562)
231. Card G, Dickinson MH. 2008 Visually mediated motor planning in the escape response of *Drosophila*. *Curr. Biol.* **18**, 1300–1307. (doi:10.1016/j.cub.2008.07.094)
232. Nalbach G. 1993 The halteres of the blowfly *Calliphora I*. Kinematics and dynamics. *J. Comp. Physiol. A* **173**, 293–300. (doi:10.1007/BF00212693)
233. Faruque I, Humbert JS. 2010 Dipteran insect flight dynamics. Part 1: longitudinal motion about hover. *J. Theor. Biol.* **264**, 538–552. (doi:10.1016/j.jtbi.2010.02.018)
234. Strausfeld NJ, Seyan HS. 1985 Convergence of visual, haltere, and prosternal inputs at neck motor neurons of *Calliphora erythrocephala*. *Cell Tissue Res.* **240**, 601–615. (doi:10.1007/BF00216350)
235. Gao N, Aono H, Liu H. 2011 Perturbation analysis of 6DoF flight dynamics and passive dynamic stability of hovering fruitfly: *Drosophila melanogaster*. *J. Theor. Biol.* **270**, 98–111. (doi:10.1016/j.jtbi.2010.11.022)
236. Liu H, Nakata T, Gao N, Maeda M, Aono H, Shyy W. 2010 Micro air vehicle-motivated computational biomechanics in bio-flights: aerodynamics, flight dynamics and maneuvering stability. *Acta Mech. Sin.* **26**, 863–879. (doi:10.1007/s10409-010-0389-5)
237. Trimarchi JR, Murphey RK. 1997 The shaking-B2 mutation disrupts electrical synapses in a flight circuit in adult *Drosophila*. *J. Neurosci.* **17**, 4700–4710.
238. Fox JL, Daniel TL. 2008 A neural basis for gyroscopic force measurement in the halteres of *Holorusia*. *J. Comp. Physiol. A* **194**, 887–897. (doi:10.1007/s00359-008-0361-z)
239. Hedrick TL, Daniel TL. 2006 Flight control in the hawkmoth *Manduca sexta*: the inverse problem of hovering. *J. Exp. Biol.* **209**, 3114–3130. (doi:10.1242/jeb.02363)
240. Taylor GK, Thomas ALR. 2003 Dynamic flight stability in the desert locust *Schistocerca gregaria*. *J. Exp. Biol.* **206**, 2803–2829. (doi:10.1242/jeb.00501)
241. Taylor GK, Zbikowski R. 2005 Nonlinear time-periodic models of the longitudinal flight dynamics of desert locusts *Schistocerca gregaria*. *J. R. Soc. Interface* **2**, 197–221. (doi:10.1098/rsif.2005.0036)
242. Ristroph L, Bergou AJ, Ristroph G, Coumes K, Berman GJ, Guckenheimer J, Wang ZJ, Cohen I. 2010 Discovering the flight autostabilizer of fruit flies by inducing aerial stumbles. *Proc. Natl Acad. Sci. USA* **107**, 4820–4824. (doi:10.1073/pnas.1000615107)
243. Fry SN, Sayaman R, Dickinson MHM. 2003 The aerodynamics of free-flight maneuvers in *Drosophila*. *Science* **300**, 495–498. (doi:10.1126/science.1081944)
244. Sun M, Xiong Y. 2005 Dynamic flight stability of a hovering bumblebee. *J. Exp. Biol.* **208**, 447–459. (doi:10.1242/jeb.01407)
245. Gao N, Liu H. 2010 A numerical analysis of dynamic flight stability of hawkmoth hovering passive dynamic stability of a hovering fruitfly: a comparison between linear and nonlinear methods. *J. Biomech. Sci. Eng.* **5**, 591–602. (doi:10.1299/jbse.5.591)
246. Taylor GK. 2001 Mechanics and aerodynamics of insect flight control. *Biol. Rev. Camb. Phil. Soc.* **76**, 449–471. (doi:10.1017/S1464793101005759)

247. Taylor GK, Thomas ALR. 2002 Animal flight dynamics. II. Longitudinal stability in flapping flight. *J. Theor. Biol.* **214**, 351–370. (doi:10.1006/jtbi.2001.2470)
248. Sun M, Yu X. 2006 Aerodynamic force generation in hovering flight in a tiny insect. *AIAA J.* **44**, 1532–1540. (doi:10.2514/1.17356)
249. Aono H, Liu H. 2008 A numerical study of hovering aerodynamics in flapping insect flight. In *Bio-mechanisms of swimming and flying* (eds N Kato, S Kamimura), pp. 179–191. Tokyo, Japan: Springer.
250. Xiong Y, Sun M. 2008 Dynamic flight stability of a bumblebee in forward flight. *Acta Mech. Sin.* **24**, 25–36. (doi:10.1007/s10409-007-0121-2)
251. Sun M, Wang JK, Xiong Y. 2007 Dynamic flight stability of hovering insects. *Acta Mech. Sin.* **23**, 231–246. (doi:10.1007/s10409-007-0068-3)
252. Taha HE, Hajj MR, Nayfeh AH. 2012 Flight dynamics and control of flapping-wing MAVs: a review. *Nonlinear Dyn.* **70**, 907–939. (doi:10.1007/s11071-012-0529-5)
253. Schenato L. 2003 Analysis and control of flapping flight: from biological to robotic insects. PhD Dissertation University of California, Berkeley, CA.
254. Xinyan D, Schenato L, Wei Chung W, Sastry SS, Deng X, Schenato L, Wu WC, Sastry SS. 2006 Flapping flight for biomimetic robotic insects: part I-system modeling. *IEEE Trans. Robot.* **22**, 776–788. (doi:10.1109/TRO.2006.875480)
255. Zbikowski R, Ansari SA, Knowles K. 2006 On mathematical modelling of insect flight dynamics in the context of micro air vehicles. *Bioinspir. Biomim.* **1**, R26–R37. (doi:10.1088/1748-3182/1/2/R02)
256. Aono H, Liu H. 2013 Flapping wing aerodynamics of a numerical biological flyer model in hovering flight. *Comput. Fluids* **85**, 85–92. (doi:10.1016/j.compfluid.2012.10.019)
257. Cheng B, Deng X, Hedrick TL. 2011 The mechanics and control of pitching manoeuvres in a freely flying hawkmoth (*Manduca sexta*). *J. Exp. Biol.* **214**, 4092–4106. (doi:10.1242/jeb.062760)
258. Muijres FT, Elzinga MJ, Iwasaki NA, Dickinson MH. 2015 Body saccades of *Drosophila* consist of stereotyped banked turns. *J. Exp. Biol.* **218**, 864–875. (doi:10.1242/jeb.114280)
259. Iams S. 2012 Free flight of the mosquito *Aedes aegypti*. arXiv:1205.5260.
260. Hedrick TL, Usherwood JR, Biewener AA. 2007 Low speed maneuvering flight of the rose-breasted cockatoo (*Eolophus roseicapillus*). II. Inertial and aerodynamic reorientation. *J. Exp. Biol.* **210**, 1912–1924. (doi:10.1242/jeb.002063)
261. Ristroph L, Berman GJ, Bergou AJ, Wang ZJ, Cohen I. 2009 Automated hull reconstruction motion tracking (HRMT) applied to sideways maneuvers of free-flying insects. *J. Exp. Biol.* **212**, 1324–1335. (doi:10.1242/jeb.025502)
262. Taha HEHE, Tahmasian S, Woolsey CA, Nayfeh AHAH, Hajj MRMR. 2015 The need for higher-order averaging in the stability analysis of hovering, flapping-wing flight. *Bioinspir. Biomim.* **10**, 016002. (doi:10.1088/1748-3190/10/1/016002)
263. Elzinga MJ, van Breugel F, Dickinson MH. 2015 Strategies for the stabilization of longitudinal forward flapping flight revealed using a dynamically-scaled robotic fly. *Bioinspir. Biomim.* **9**, 025001. (doi:10.1088/1748-3182/9/2/025001)
264. Elzinga MJ, Dickson WB, Dickinson MH. 2012 The influence of sensory delay on the yaw dynamics of a flapping insect. *J. R. Soc. Interface* **9**, 1685–1696. (doi:10.1098/rsif.2011.0699)
265. Doman DB, Oppenheimer MW, Sigthorsson DO. 2010 Wingbeat shape modulation for flapping-wing micro-air-vehicle control during hover. *J. Guid. Control. Dyn.* **33**, 724–739. (doi:10.2514/1.47146)
266. Oppenheimer MW, Doman DB, Sigthorsson DO. 2011 Dynamics and control of a biomimetic vehicle using biased wingbeat forcing functions. *J. Guid. Control. Dyn.* **34**, 204–217. (doi:10.2514/1.49735)
267. Zhang J, Cheng B, Yao B, Deng X. 2015 Adaptive robust wing trajectory control and force generation of flapping wing MAV. In *Robotics and Automation (ICRA), 2015 IEEE Int. Conf., Seattle, WA, 26–30 May*, pp. 5852–5857. Piscataway, NJ: IEEE.
268. Chirarattananon P, Ma KY, Wood RJ. 2014 Adaptive control of a millimeter-scale flapping-wing robot. *Bioinspir. Biomim.* **9**, 25004. (doi:10.1088/1748-3182/9/2/025004)
269. Chirarattananon P, Ma KY, Wood RJ. 2014 Fly on the wall. In *Biomedical Robotics and Biomechatronics (20145th IEEE RAS & EMBS) Int. Conf., Sao Paulo, Brazil, 12–15 August*, pp. 1001–1008. Piscataway, NJ: IEEE.